Theoretical Study on Molecular Networks of Carbon Dioxide to Methanol Conversion

Ph.D. Dissertation

Rachid Hadjadj

Supervisor:
Prof. Dr. Béla Viskolcz

Antal Kerpely Doctoral School of Materials Science & Technology

Institute of Chemistry

University of Miskolc

Miskolc 2020

"But over all those endowed with knowledge is the All-Knowing"

The Noble Qur'an [Chapter 12-Yusuf, Verse 76]

Contents

Acknowledgments

My doctorate would not have been possible without the help of many people whom I would like to thank here.

I deeply thank Prof. Dr. Béla Viskolcz, my thesis director, for his advices, for his indestructible confidence and optimism and for giving me the opportunity to work within his team on a topical subject.

I am very happy for having frequent meetings with a great Hungarian mind, a person that gave me the feeling of having a grandfather again! Prof. Imre G. Csizmadia, the most brilliant person I have talked to. Thank you for your help, your hospitality, and humour.

A big thank you to a person whom I consider as my older brother, Dr. Béla Fiser, not only for his daily scientific help, but for being the first person I think about knocking the door in all circumstances.

Thanks to Dr. Michael Owen for proofreading this dissertation.

Thanks to Dr. Szőri Milan for everything he taught me during my thesis period.

Thanks to the administrative team, Vanczákné Jutka in particular, for all the help and for her smile.

Thanks to Edina Reizer for being such a good friend.

I would like to thank my family members and friends in French.

Papa, merci pour ton soutien constant, j'ai toujours rêvé de porter le nom de Dr. Hadjadj après toi, voilà que ça se réalise enfin. El-hamdou li allah.

Mama, merci pour ton amour éternel et pardon de t'avoir fait endurer la douleur de mon éloignement.

Sid Ahmed et Amine, mes frères bien-aimés, de tout mon cœur, je nous souhaite à tous les trois un magnifique avenir commun. Sachez que je suis fière de vous.

Merci à mes trois meilleurs amis, Dr. Sid Ahmed Kessas, Dr. Mohamed El-Bachir Belaid et M. Yacine Sardi, d'être mes meilleurs amis pendant près d'une décennie.

Merci aux amis que j'ai rencontré ici en Hongrie : Gacem Walid, Benchabane Mehdi, Mehdi Yacine et Dib Amine.

Je dédie particulièrement ce travail à une personne très importante pour moi, une personne qui n'est plus de ce monde, le directeur de ma thèse de Master, le Prof. Kessas Rachid. Vous êtes probablement la personne que je voulais le plus me voir obtenir le titre de docteur. Je suis

tellement fier d'être la dernière personne que vous avez encadré dans votre vie. Vous êtes la personne qui m'a fait choisir la recherche scientifique. J'espère que je suivrai votre chemin.
Si seulement j'ai pu vous dire tout ça la dernière fois que nous nous sommes parlé…

This research was supported by the European Union and the Hungarian State, co-financed by the European Regional Development Fund in the framework of the GINOP-2.3.4-15-2016-00004 project, aimed to promote the cooperation between the higher education and the industry.

List of figures

List of tables

Abbreviations

ΔG_r^o: Gibbs free energy of a reaction.

ΔH_r^o: Heat of a reaction.

ΔH_f^o: Heat of Formation of species.

$\Delta G°$: Relative Gibbs free energy.

$\Delta H°$: Relative enthalpy.

$\Delta S°$: Relative entropy.

ΔE_{tot}: Total energy change.

η: Efficiency.

B3LYP: Becke, 3-parameter, Lee-Yang-Parr method.

CC: Coupled cluster methods.

CCS: Carbon Capture and Storage.

CCU: Carbon Capture and Usage.

CI: Configuration interaction method.

CPCM: Conduction-like Polarizable Continuum Model.

DFT: Density functional theory.

G_{ref}: Gibbs free energy of the reference species.

G(X): Gibbs free energy of structure X.

GTO: Gaussian-type orbitals

HF: Hartree-Fock method.

MD: Molecular Dynamics.

MEA: Monoethanolamine.

MM: molecular mechanics.

MP: Møller–Plesset perturbation.

MPa: Mega pascal.

Mtoe: Million tonnes oil equivalent.

Mt: Million tonnes.

MW: Megawatt.

PES: Potential energy surface.

pK_a: Acid dissociation constant.

PCM: Polarizable Continuum Model.

RMSD: Root Mean Square deviation.

RWGS: Reverse-Water Gas Shift.

Rx: Chemical reaction number x,

***S*:** Entropy.

SCRF: Self Consistent Reaction Field.

SNG: Substitute Natural Gas.

TS: Transition State.

TWh: Terawatt hour.

QCISD: Quadratic Configuration Interaction including Single and Double substitutions.

Wn: Weizmann-n method.

W1BD: Brueckner Doubles variation of the Weizmann 1 method (W1).

W1U: Unrestricted variation of the Weizmann 1 method.

WHSV: Weight hourly space velocity.

1 Introduction

“Two things are infinite: the universe and human stupidity; and I'm not sure about the universe.”
Albert Einstein

1.1 Historical background

People who are interested in human history are usually classified into two groups, the ones who are interested in the history of past are called *historians*, and the other group which is interested in the future and are called *futurologists*. In this dissertation we discuss energy production and transformation, which was started about four centuries ago with the invention of the steam engine. This *historical background* influenced climate change. In contrast to that there is the *futuristic aspect* of energy production, which could be based on atomic nuclear fusion. Such a technique could be operational in the second half of the twenty-first century, perhaps as early as 2050. By then, several European countries are aiming to reach carbon neutrality (net zero carbon dioxide emissions)[1]. Between the *historic aspect* of the 'carbon-based' past and the *futuristic aspect* of our possible 'nuclear-based' future, there must be a *transition period*. In this case the most important challenge during this *transition* could be the chemical reduction of CO_2 to more useful compounds (**Figure 1**).

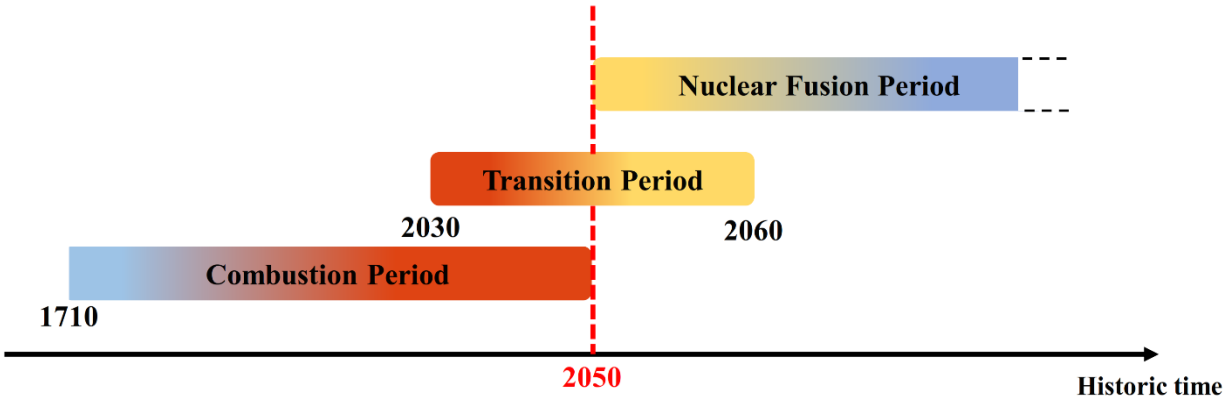

Figure 1: Energy production types through history.

During the current industrial phase of the global civilization, energy production is mainly based on combustion (**Figure 1**, left). Sooner or later, this method will be replaced by nuclear fusion (**Figure 1**, right), until then, we must get through a transition period (**Figure 1**, middle) in the near future, within which the world must focus on CO_2 management.

1.2 Trend of the energy sector

According to the Statistical Review of World Energy consumption created by British Petroleum (BP)[2], the growth of the world population is reflected in an increasing energy demand of all the economic branches. Consequently, the annual consumption of primary energy in the world is constantly increasing (**Figure 2**).

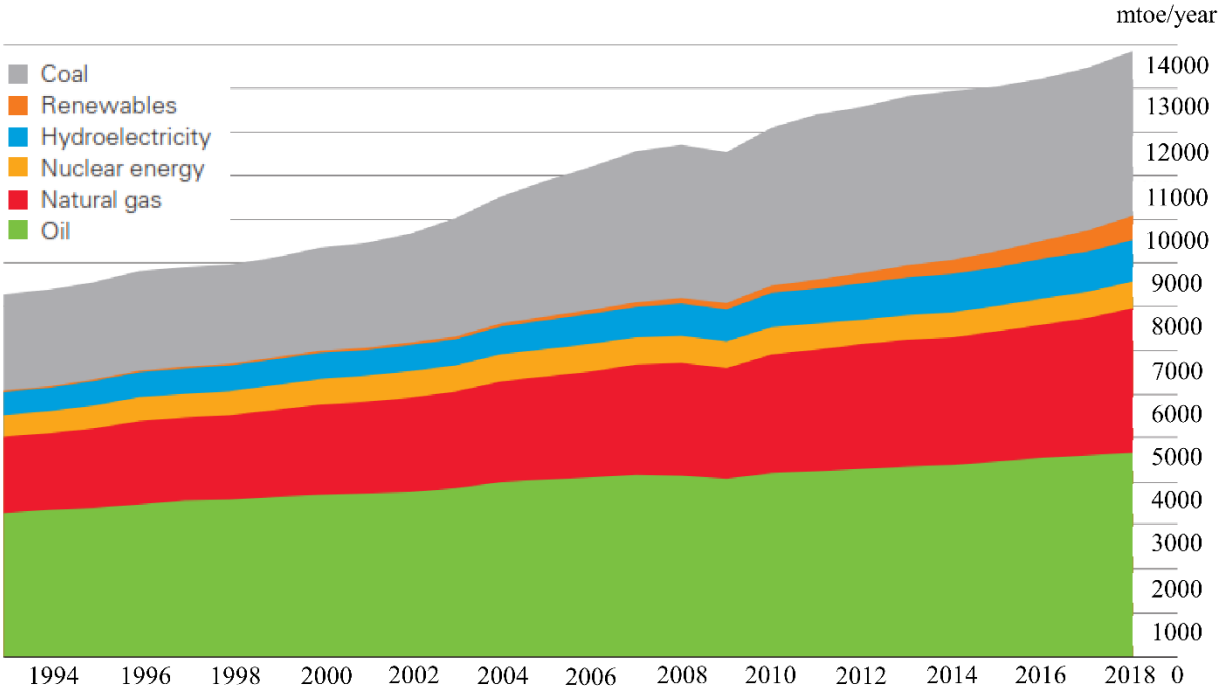

Figure 2 Global energy consumption between 1990 and 2018 in million tonne of oil equivalent[2].

The primary global energy consumption in the world do not stop increasing (**Figure 2**). The total energy consumed in the year 2018 is equal to **13864.9** million tonne of oil equivalent (**mtoe**)**.** The growth rate of the global energy consumption is **2.9%** in 2018**.** It is the double of the "10-year growth increasing average" of **1.5%** and is the fastest since 2010. Oil, natural gas, and coal are the most consumed fuels in the world (**Figure 2**), whereas the rate of natural gas consumption is increasing the fastest, as demonstrated by its **40%** increase. Of course, the consumption of each fuel grew, and renewables and hydroelectricity were not exceptions[2].
With limited fossil-fuel resources, asking the question of which new sources of energy will be most suitable for the future is unavoidable. It is certain that the growth in energy demand will continue especially in emerging countries and eliminating carbon dioxide from the equation of the power sector is perhaps the most important challenge facing the global energy system over the next 30 years.

1.3 The energetic transition

Energy, the basic element that every nation need, is now being intensely investigated and being probed by the scientific world in order to find its sustainable forms[3]. Declining energy resources combined with its increasing demand, as well as the environmental impact (global warming and climate change) led to what is called "Energetic Transition". Energetic transition is nothing but the progressive replacement of fossil-fuel energy sources (oil, natural gas, coal) by renewable energy sources (solar energy, wind energy, water energy, biomass).

1.3.1 Biofuels

As an alternative of fossil fuels, biofuels are produced from biomass through contemporary processes. They can be produced from plants, or from agricultural, commercial, domestic, and/or industrial wastes of biological origin)[4].

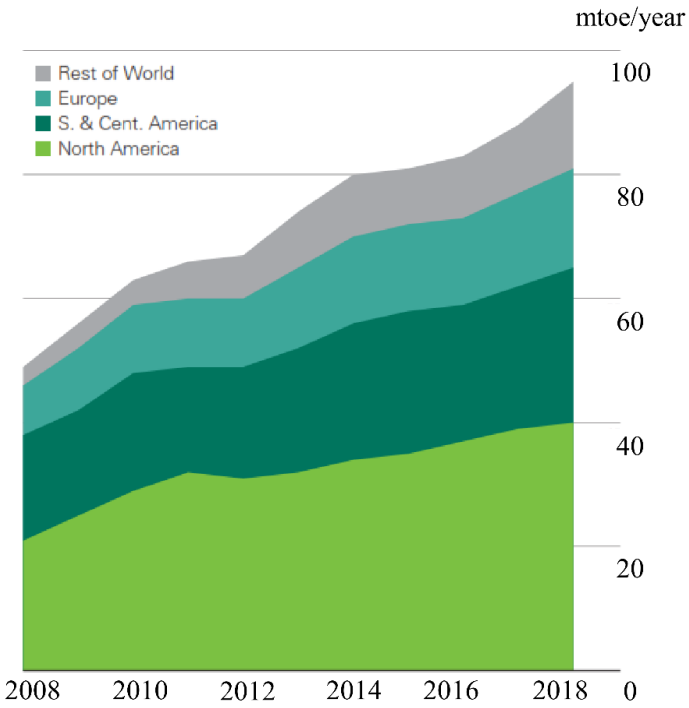

Figure 3: Biofuel production in different regions[2].

From 2012, more and more biofuels were produced each year (**Figure 3**). The total world production reached **95371 mtoe** in 2018. North America (**39.5 mtoe**) is the largest producer in the world, followed by South and Central America (**25.5 mtoe**), Europe (**15.9 mtoe**), and then the rest of the world.

The average growth of biofuel production reached **9.7%** in 2018, which is the highest growth since 2010 and slightly above the 10-year average[2]. Though biofuels have a number of

advantages over fossil fuels, their integration into the fuel supply chain has some limitations. In fact, the production of biofuels requires growing crops, which means that an excessive use of water will be needed, and the use of fertilizers. In addition to that, crops cannot grow in every region of the globe. Also, the amount of biofuel produced in the world is almost negligible compared to the total energy consumed.

1.3.2 Hydrogen based electricity

Hydrogen fuel is considered as a zero CO_2 emission fuel while it reacts with oxygen. It is mainly used in fuel cells and internal combustion engines. It has been adapted to function in vehicles such as cars and buses for many years. It is also used as a fuel for spacecraft propulsion[5].

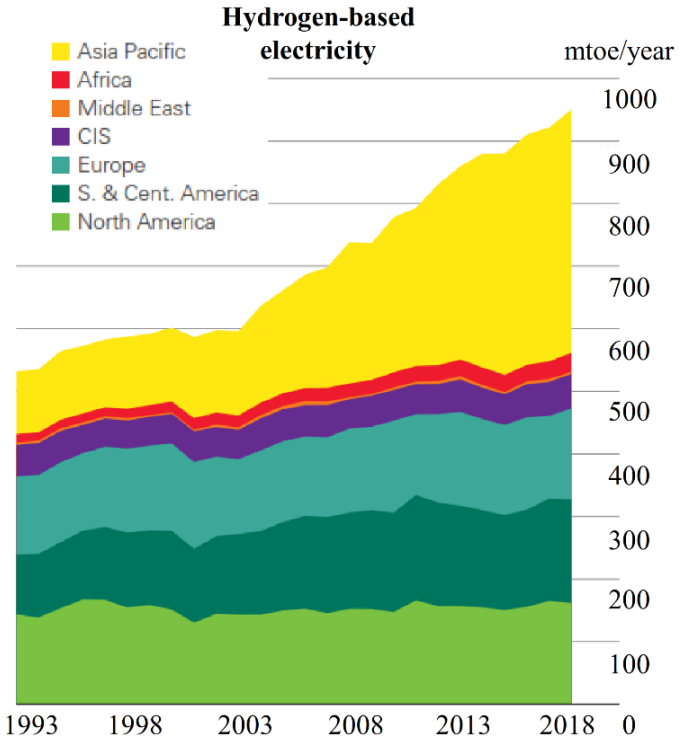

Figure 4: Hydrogen based electricity consumption[2].

The production of electricity from hydrogen-based processes is also growing (**Figure 4**). The world has consumed **948.8 mtoe** of hydrogen-based energy in 2018 and its production trend suggests that this will continue to increase.

1.3.3 Nuclear-based electricity

To generate nuclear power, nuclear reactions have to be used for the release of nuclear heat energy, which is used in steam turbines to produce electricity in a nuclear power plant. In addition to all the risks of disastrous nuclear explosions, the nuclear plants generate radioactive nuclear waste, which might can have a detrimental effect on the human race for generations. Thus, scientists are turning to developing nuclear fusion instead of the fission of uranium and plutonium[6].

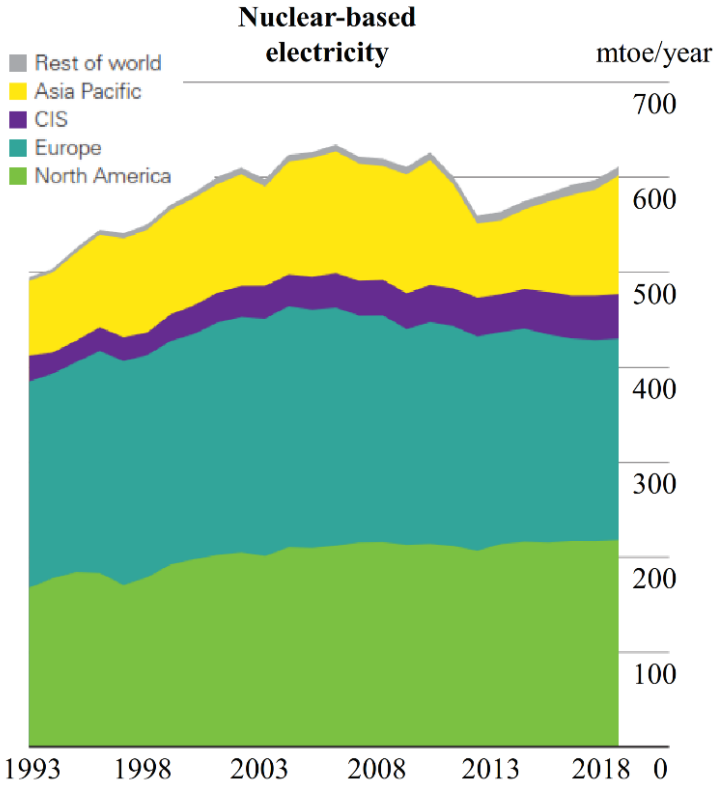

Figure 5: Nuclear-based electricity consumption[2].

Global nuclear-based energy consumption increased at a rate of **2.4%** since 2013, reaching **611.3 mtoe** in 2018. However, during the last 25 years, it has been continuously fluctuating. For example, the amount consumed in 2018 is lower than that consumed in 2006 (**Figure 5**). This type of energy production has still not reached sustainability.

1.3.4 Renewable energies

Renewable energy has a vital role to play in meeting the challenge of eliminating CO_2 emissions. Nevertheless, its production is not stable, and depends highly on the weather and other factors. Given that energy consumption fluctuates drastically as well, the development of various energy storage procedures also necessary[7].

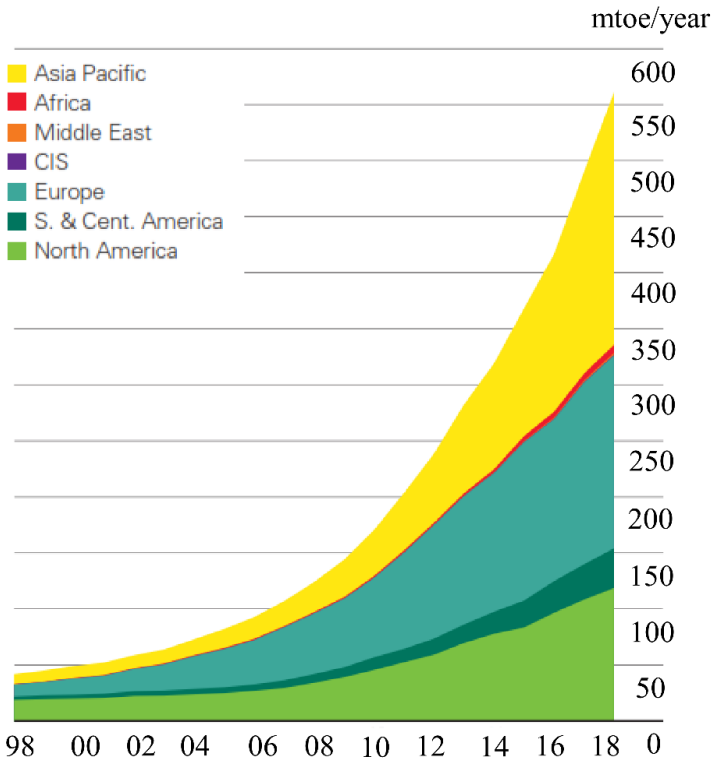

Figure 6: Renewable energy consumption[2].

Renewable energy consumption exponentially increases in different locations of the world (**Figure 6)**. Renewables sources of energy are promoted to be the most favorable substitute for fossil fuels. Asia-Pacific areas of the word seems to lead in terms of the renewable energy amounts consumed (**225.4 mtoe)** followed by Europe (**172.2 mtoe**) and North America (**118.8 mtoe).** Interesting to note that the largest concentrated solar farm is located in Morocco, which is called Noor (meaning light in Arabic).

In 2018, renewable energy in power generation (excluding hydro) increased by **14%**, slightly below the 10-year average growth (**16%**). China alone contributed in **45%** of the global growth.

Compared to solar energy (**131 TWh**), wind contributed more to the growth of renewable energy (**142 TWh**), and it has accounted for around **50%** of the renewable energy generated in the last few years. Solar has constantly increased its share and now represents **24%**.

1.3.5 Energy storage problem

Although there are several ways to store energy, not all of them have the same storage capacity and duration (**Figure 7**).

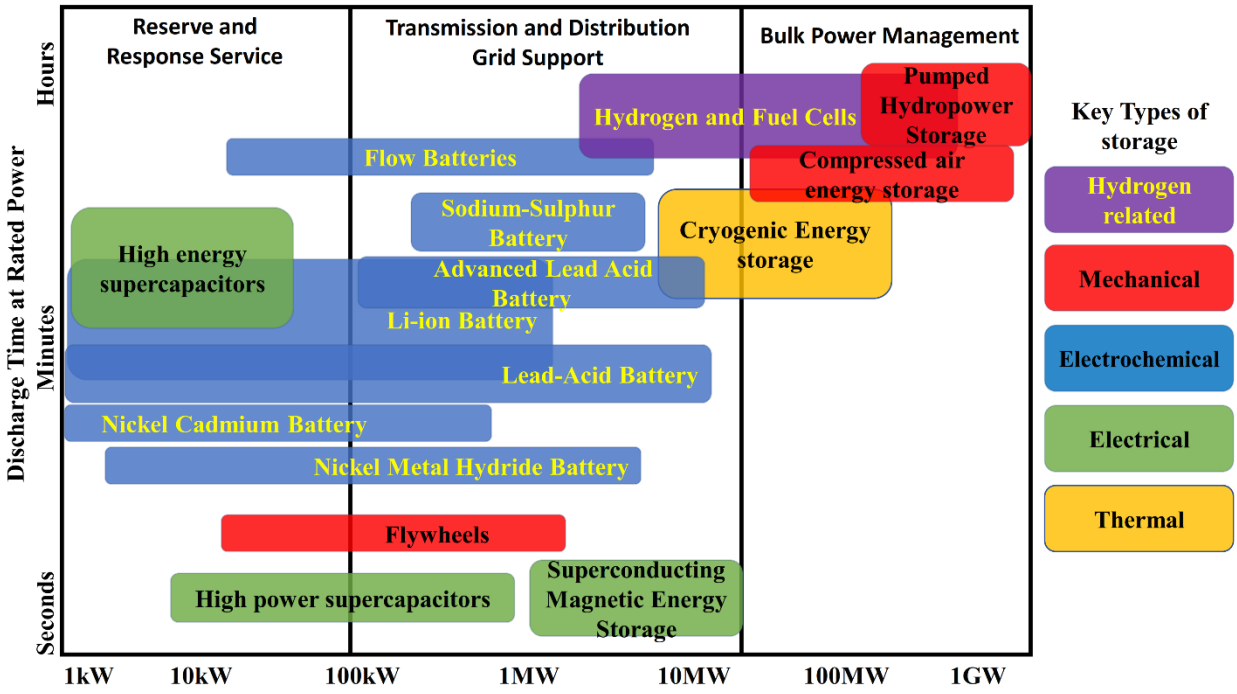

Figure 7: Characteristics of different energy storage types[8].

Batteries are the most used devices for energy storage. The storage power and the discharge time can vary according to their type. Flywheels, high power superconductors and the magnetic energy storage methods have the lowest potential for energy storage. The best energy storage methods are the compressed energy storage systems, the pumped hydrogen power systems and the hydrogen fuel cells because of their ability to store high quantities of energy for a long time.

It is important to note that large-capacity energy storage methods are badly needed in order to support the extensive use of renewable electricity. The renewable electricity production strongly depends on the weather, and thus, its production is highly fluctuating. Unfortunately, the electricity consumption is also fluctuating, but in a different way. Therefore, the storage problem of renewable electricity should be solved[7]. The high capacity of energy storage can be completed with Substitute Natural Gas (SNG). Storing energy in chemical bonds by recycling of carbon dioxide via hydrogenative reductions can be the most convenient way of storing renewable electrical energy[9].

1.4 CO_2 management

The aim of energy transition is to reduce CO_2 emissions. The valorization of this molecule presents an additional opportunity to achieve this goal. Instead of letting carbon dioxide escape into the atmosphere, it can be captured where it is generated such as the industrial or

biochemical processes[10]. Then, through chemical transformations, added-value molecules can be created allowing it to be recycled. This process is called Carbon Capture and Usage (CCU)[11].

1.4.1 CO_2 emission and climate change

The harmful effect of carbon dioxide emitted into the atmosphere is a well-known issue, and research in environmental protection is a challenge nowadays[12]. CO_2 emissions continue to increase as shown in **Figure 8,** as a result of the consumption of fossil fuels[13], which is one of the factors behind global warming and the acidification of the oceans[14].

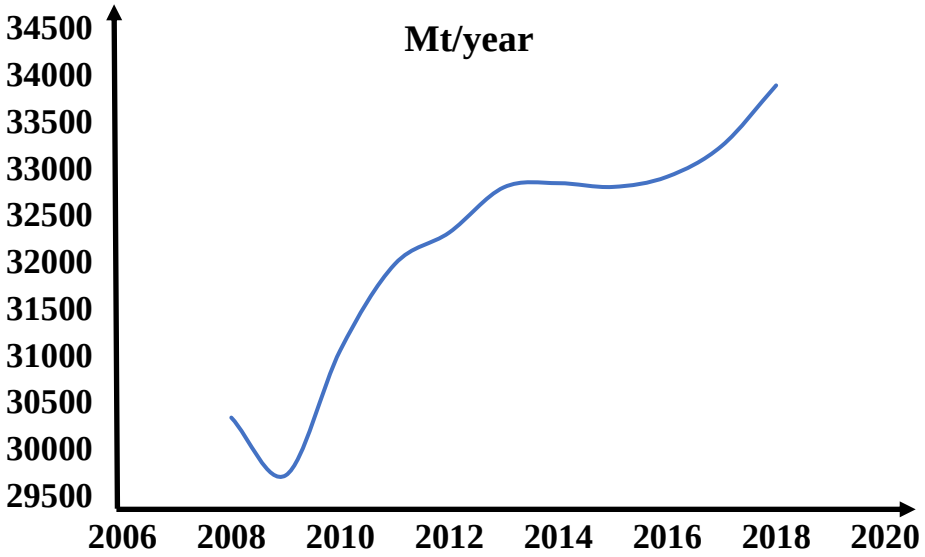

Figure 8: World CO_2 emission in the 2008-2018 time period[2].

From **Figure 8** we notice that since 2009 the amount of global CO_2 emissions is continuously increasing and it reached **33890.8 Mt** in 2018 with a growth rate of **2.0%**, which is the fastest in the last seven years.

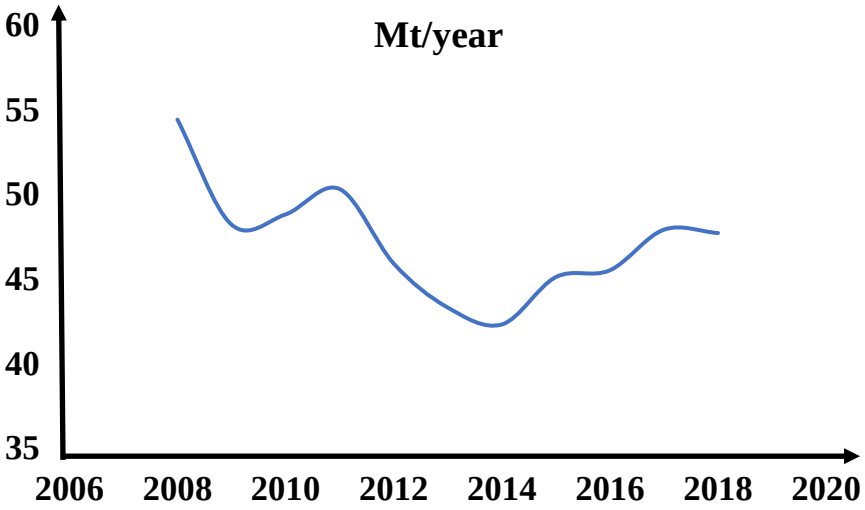

Figure 9: CO_2 emission in Hungary between 2008-2018[2].

In Hungary, the CO_2 emission seems to be fluctuating between **50.3 Mt** and **42.3Mt** except for the year 2008 where the emissions reached the highest value **54.4 Mt** as shown in the **Figure 9**.

1.4.2 CO_2 and economy

An increasing and successful economy requires an increasing amount of energy production, which in the current 'combustion period' means an increasing production of CO_2. Reducing the present production rate could lead to an economic collapse unless different energy production methods are introduced. In the meantime, serious efforts must be made to reduce CO_2 emission and its concentration in the atmosphere[9].

1.4.3 Carbon Capture and Storage (CCS)

Most of the solutions proposed to reduce CO_2 emissions until now are mainly Carbon Capture and Storage (CCS) methods[15] which are not definitive solutions to eradicate the excess of CO_2 from the atmosphere[16]. For example, some ocean scientists think that ocean storage of CO_2 might be a good idea. In this case, the gas would be injected and trapped into the deep ocean[17], but it is unlikely to remain there permanently.

1.4.4 Carbon Capture and Usage (CCU) as potential energy storage methods

From a chemical point of view, the best solution would be the total transformation of carbon dioxide into products that have higher value[18,19], and in this way the produced renewable energy can also be stored[20]. It could be used to carry out the reactions and convert carbon dioxide chemically into different molecules for the sake of energy storage[21]. These molecules can be used not only for the storage and production of energy, but to produce other chemicals in a renewable basis[22]. The necessary hydrogen could be obtained from the electrolysis of water using renewable electrical energy[23], or steam reforming of natural gas[24] which should contribute to the decrease of CO_2 emission[9].

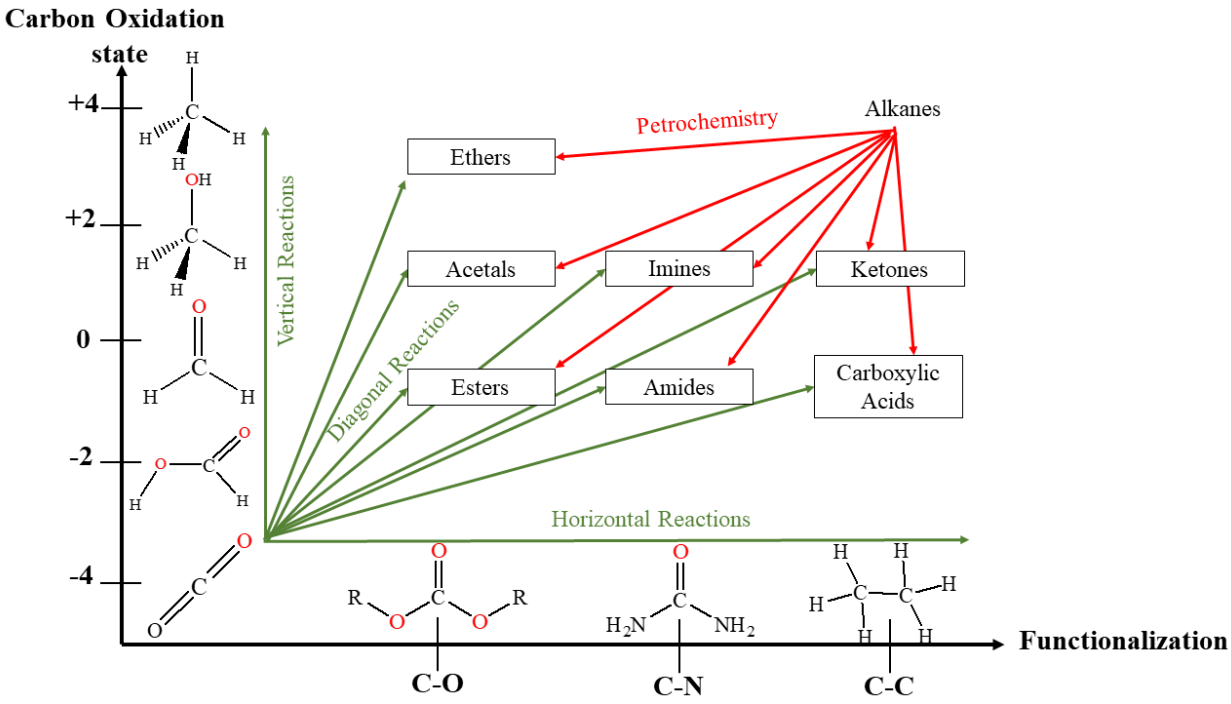

Figure 10: CO_2 Valorisation by chemical reactions.

A more feasible option to handle CO_2 could be using it as a reactant in the formation of more complex molecules such as polycarbonates, urea and alkenes. The ability to use these molecular end products in other processes is indicative of their increasing value, and can thus be considered an added-value product compared to CO_2, which is essentially an unwanted by-product of combustion and a strong contributor to global warming and climate change. (**Figure 10**). Such an application would decrease the amount of CO_2 released into the atmosphere and significantly reduce the carbon footprint associated with economic development in these, the last days of the combustion era and the beginning of our energy transition period towards more sustainable energy sources.

By the hydrogenation of CO_2, energy can be stored in chemical bonds (**Figure 10**). The reduction of carbon dioxide could lead to formic acid, formaldehyde, methanol and methane by decreasing the oxidation state of carbon.

Extensive research efforts have been made to find novel methods for CO_2 recycling. In order to produce hydrocarbons which are used as fuels and basic reagents to synthesize other chemicals in a competitive manner to petrochemistry, reduction and the formation of new C-C, C-O and C-N bonds were combined. For example, methanol is a suitable product of the reduction of carbon dioxide because of its high energy density and its ability to be reintroduced into other chemical processes as feedstock to produce more advanced chemical compounds[19].

It is expected that methanol will play a growing role in future non-fossil fuels and getting it from the valorization of carbon dioxide is very promising[21].

1.5 The methanol synthesis

Between the different methanol production processes, CO_2 can be reduced chemically, or introduced first in a reverse water-gas shift reaction (RWGS) as a fraction of synthesis gas[25]. In the last decades CO_2 hydrogenation to methanol has been a widespread subject of interest, large variety of solid catalysts have been designed and tested[26]. However, the reduction mechanism is still a debated subject and new processes are proposed[27].

1.5.1 Route of CO_2 reduction

The reduction involves the uptake of a hydrogen atom, a process which may be achieved by electrochemical reaction or by catalytic hydrogenation (**Figure 11**).

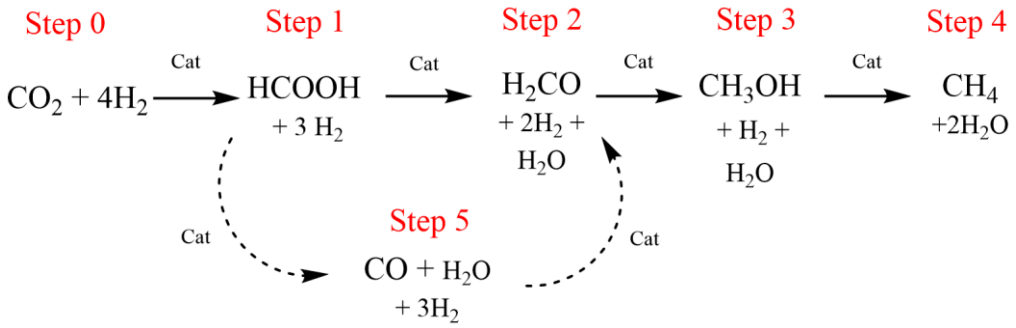

Figure 11: Stepwise reaction of carbon dioxide hydrogenation to achieve methanol and methane. Cat refers to catalytic reaction. The dashed arrows represent side reactions.

The reduction stages of CO_2 can be described by the production of three isolatable intermediates, such as HCOOH, H_2CO, CH_3OH and the final product, CH_4[28]. Step 5 can be considered as a side reaction where through two steps carbon monoxide is formed as an extra intermediate.

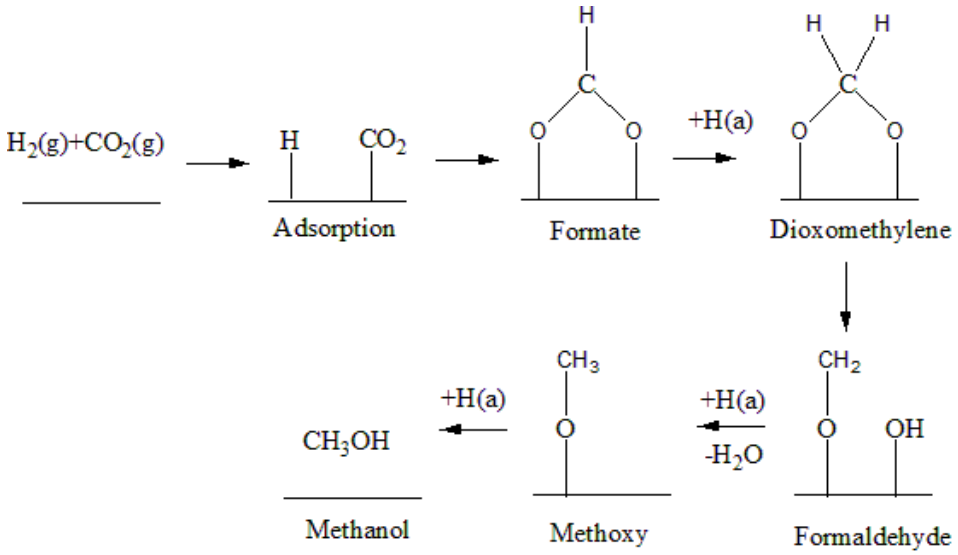

Figure 12: Proposed reaction mechanism for the synthesis of methanol from CO_2 on Cu[29].

Most of the mechanisms proposed for the synthesis of methanol on the surface of Cu catalysts only describe the metal-bound phase (**Figure 12**)**.** After the adsorption of CO_2 and hydrogen, formate is formed. It is generally considered to be the most stable intermediate. Then, by the successive hydrogenation of intermediates, formate is transformed into methoxy before undergoing a final hydrogenation into methanol.

1.5.2 Side reactions

Several side reactions (*e.g.* leading to hydrocarbons) could also occur during the hydrogenation of CO_2. CO_2 and H_2 are considered as synthesis gas that can produce complex hydrocarbons. The simplest hydrocarbons in this case are expected to be ethylene and ethane.

At this stage it might be reasonable to point out that the following possible side reaction:

$$2\ CO_2 + 6\ H_2 \longrightarrow H_2C{=}CH_2 + 4\ H_2O \qquad (\mathbf{R1})$$

will lead to a valuable product (ethylene) which is a monomer for polyethylene formation, and it is very useful for other purposes in the chemical industry.

1.5.3 Catalysts

The nature of the catalyst is a key question both in terms of its effectiveness and in terms of how many of the 4 main steps (**Figure 11**) can be catalyzed in order to increase the rate of the formation of the targeted product while avoiding side products. In the following section, we have focused mainly on these two questions.

The catalysts used for CO_2 transformation are mostly metal-based systems. These systems can be divided into two groups, copper-based catalysts, and catalysts based on Au, Pd, $Ni_{(x)}In_{(y)}$ or NiGa (**Table 1** and **Table 2, respectively**).

Table 1: The performance of Cu-based catalysts in the conversion of CO_2 to methanol.

Catalyst	T (°C)	P (Mpa)	H_2:CO_2	WHSV ($mL.g^{-1}.h^{-1}$)	CO_2 Conversion (%)	CH_3OH selectivity (%)	Ref.
Cu/ZnO	250	3.0	3:1	18000	11.0	-	30
Cu/ZrO_2	260	8.0	3:1	3600	15.0	86.0	31
CuO/ZnO	250	2.0	3:1	3750	8.6	45.0	32
$Cu/ZnO/Al_2O_3$	270	5.0	3:1	4000	23.7	43.7	33
$Cu/ZnO/Al_2O_3/ZrO_2$	190	5.0	3:1	4000	10.7	81.8	34
$Cu/ZnO/Al_2O_3/Y_2O_3$	230	9.0	3:1	10000	29.9	89.7	35
$Cu/ZnO/ZrO_2/AlO_3/SiO_2$	250	5.0	2.8:1	10000	-	89.7	36
$Cu/ZnO/Ga_2O_3/$	240	4.5	2.8:1	18000	27.0	50.0	37
Cu/TiO_2	260	3.0	3:1	3600	-	64.7	38
Cu/ZrO_2/CNTs	260	3.0	-	3600	16.3	43.5	39
CuZnO/Ui-bpy	250	4.0	3:1	18000	3.3	100.0	40

A wide variety of copper-based catalysts have been used to convert CO_2 to methanol (**Table 1**). The operating conditions are varied, but the temperature (T) and the ratio of the reactants was in most cases around 250 °C and 3:1 (H_2:CO_2), respectively. The pressure (P) varied between 3-9 MPa, and there was no special value applied for the Weight Hourly Space Velocity (WHSV). The results of the experiments were evaluated mainly by the conversion rate and selectivity of the final product. In five of the cases the selectivity was over 80%, and in the case of (CuZnO/Ui-bpy) it even reached 100%. However, the conversion yield was the lowest in this case (3.3%). In the case of the conversion parameter among all the catalysts, the highest measured value observed in literature is 29.9%, and it belongs to the $Cu/ZnO/Al_2O_3/Y_2O_3$ system where the selectivity was equal to 89.7%.

Table 2: The performance of Au, Pd, NiIn and NiGa catalysts in CO_2-methanol conversion.

Catalyst	T (°C)	P (Mpa)	H_2:CO_2	WHSV (mL.g^{-1}.h^{-1})	CO_2 Conversion (%)	CH_3OH selectivity (%)	Ref.
Au/ZnO	240	0.5	3:1	-	0.4	49.0	41
Au/ZnO	240	5.0	3:1	-	1.0	70.0	41
Pd/ZnO	250	2.0	3:1	3600	11.1	59.0	42
Pd/ZnO/TiO_2	250	2.0	3:1	3600	10.1	40.0	43
PdZnO/CNFs	275	0.1	9:1	7500	3.3	12.1	44
PdCuZnO/SiC	200	0.1	9:1	7500	-	80.9	45
Pd/Plate Ga_2O_3	250	5.0	3:1	6000	17.3	51.6	46
$Ni_{3.5}In_{5.3}Al/SiO_2$	260	0.1	3:1	12000	3.8	2.3	47
NiGa/SiO_2	250	0.1	3:1	-	-	98.3	48
Pd/Mo_2C	135	-	3:1	-	-	95.0	49
Pd/In	190	-	3:1	-	-	94.0	50

In the case of the non-Cu-based catalysts (**Table 2**), a pressure and temperature between 0.1 to 5 MPa, and 200 to 275 °C was required. The ratio was kept in most of the cases to 3:1. The conversion in these cases was not excellent: the highest value was achieved in the case of the Pd/plate Ga_2O_3 system (17.3%). The highest selectivity is 98.3% and it was achieved with the NiGa/SiO_2 catalyst, but in this case the conversion rate is not mentioned.

The catalysts currently used most often in industry are copper-based, thermally stable materials due to the use of alumina as a support structure , are mainly optimized for mixtures of synthesis gas (H_2, CO and CO_2), and are generally issued from natural gas reforming process.

1.5.4 Industrial processes for methanol production

The worldwide methanol production is mainly dominated by a few companies. The Imperial Chemical Industries (ICI) is accounting for 61% of the installed capacity with the Synetix process, and the Lurgi process for 27%[9]. Other processes exist such as the Mitsubishi Gas Company (MGC) process, but the main differences between all them remain in the type of the reactor design and the catalyst disposure (fixed bed reactor, fluidized bed reactor, tubular reactor…)[9]. Most current methanol production companies use methane as feed stock. Through hydrocracking, methane is transformed to syngas (mainly CO_2, H_2, CO) which is routed directly to a reactor where the catalytic methanol reaction takes place[51].

1.6 Goal

The chemical hydrogenation of CO_2 to methanol by using renewable energies can be the key to solve the problem of renewable energy storage as well as to reduce CO_2 emissions. However, carbon dioxide hydrogenation is a mechanistically complicated multi-step process. Therefore, it is indispensable to understand the mechanism. Computational chemistry tools can be used further to understand this process.

This thesis is an assembly of three major computational chemistry studies:

- A gas phase study: where all the molecular complexes that might be formed from the (CO_2+$4H_2$) reaction mixture are investigated and the most stable ones will be selected to be part of a newly designed network for the uncatalyzed carbon dioxide hydrogenation to methanol and methane. The energetics of the elementary steps constituting the network will be studied, and the efficiency of the most favourable pathway will be calculated.

- An aqueous phase study: knowing that carbon dioxide can be absorbed by water as it happens in the oceans, an uncatalyzed water enhanced hydrogenation mechanism for CO_2 conversion to methanol will be designed and thermodynamically studied. The efficiency of the preferred pathway will be calculated and compared to the gas phase results.

- An aqueous phase catalyzed-like study: the major role of a solid catalyst in the methanol synthesis is the conversion of hydrogen molecules to hydrogen atoms (bond dissociation). To mimic this property of the catalysts, a catalyzed-like mechanism will be constructed involving hydrogen atoms instead of hydrogen molecules and studied energetically. Thereafter the efficiency will be calculated taking into account the hydrogen bond dissociation energy.

These studies aim to provide a better understanding of this difficult process, and to identify and propose mechanisms to reduce the barrier height of the rate-limiting steps under different chemical conditions that can be directly applied to industrial settings. The findings can be applied in the near future to the design and development of new special-purpose catalysts for the ‘elimination’ of CO_2 and to reduce its detrimental effects on our global ecosystem.

2 Computational methods

"The history of science shows that theories are perishable. With every new truth that is revealed we get a better understanding of nature and our conceptions and views are modified"

Nicolas Tesla (1856 – 1943)

2.1 Computational chemistry

Computational chemistry uses the basics of quantum chemistry to predict molecular properties for a better understanding of nature from a chemical point of view. It describes a system's physical properties using the wave function through the action of operators and determines through the Schrödinger equation (1) its energetic state.

$$\hat{H}\Psi = E\,\Psi \qquad (1)$$

Here $\hat{H}$ is the Hamiltonian operator which describes the kinetic and potential energies of the system. Ψ is the electronic wave function and E is the total electron energy.

Because of the vast computational demands required to solve the Schrödinger equation, many approximations are necessary. In most of the cases, quantum chemists assume that the motion of electrons is separated from that of the nuclei. In the Born-Oppenheimer approximation[52], only the electronic part is solved, whereas the nuclear part is approximated.

Thermodynamic properties (such as $\Delta_r G$, $\Delta_r H$, S, $\Delta_f H°$, pK_a) of short-lived molecules, unstable intermediates, and transition states, can be calculated using computational chemistry methods. Thus, the reaction mechanisms can be examined quantitatively, and indicate when appropriate catalysts can be designed and applied to avoid potential by-products or side reactions.

2.2 Level of theory

The different theoretical approaches which corresponds to various approximations of the electronic Schrödinger equation with a certain accuracy are called the levels of theory. It has two degrees of freedom: one is the treatment of electron correlation, and the other is the basis set.

2.2.1 Methods

2.2.1.1 Ab initio molecular orbital theory

Ab initio (from first principal in Latin) molecular orbital theory is used to predict the properties of atomic and molecular systems. It is based upon the fundamental laws of quantum mechanics and uses a variety of mathematical transformation and approximation techniques to solve the fundamental equations. the only inputs into an *ab initio* calculation are physical constants[53].

The most widely used approximation in quantum chemistry is the Hartree-Fock (HF) method[54], as it forms the basis of more sophisticated molecular orbital methods. It is based on the assumption that the Slater determinant wave function of an electron cloud can be constructed from the corresponding spin-orbital product[55] and this can be extended to any number of electrons and thus, can be used to approximate the multi-electron wave function of the system.

The HF *ab initio* method does not address electron correlation within a system, which leads to a low computational time, but also a lower computational accuracy.

To achieve higher accuracy, post-Hartree-Fock *ab initio* methods have been developed, within which the treatment of electron correlation is been included. The Møller–Plesset perturbation theory (MP)[56] is one of those which has a relatively low computational cost, but it is ideal only if the electron correlation level is relatively low. Higher order perturbation methods can be derived from the Møller-Plesset expansion when it is truncated at the second (MP2)[57], third (MP3) or fourth (MP4) order of perturbation.

Another type of post-Hartree-Fock methods is the configuration interaction (CI) method. A special correction of this is the quadratic configuration interaction with single and double substitutions or QCISD[58]. Coupled cluster methods (CC)[59] are used to describe multi-body systems constructing multi-electron wave functions and employing the exponential cluster operator to account for electron correlation. These methods apply series expansion, which results in the formation of determinants from the reference Slater determinant-like wave function, where one or more electrons are transferred to the unoccupied orbitals of the reference determinant. A drawback of this method is that it is not variational. The CCSD[60] (coupled cluster singles and doubles) method contains single and double excitations, while the CCSD(T) additionally includes the perturbative approximation of triple excitations. Currently, the CCSD(T) is the most precise electronic structure method still applicable for small systems.

2.2.1.2 Density functional theory (DFT)

The hybrid density functional theories (DFT)[61] are the most popular quantum chemical approaches used to determine the electronic structure of the molecules. Also derives from quantum mechanics but instead of using the wave function to determine the properties of multi-electron systems as it is done in ab initio methods, these methods uses the electron density function to calculate the energy using an exchange-correlation functional.

A large number of different functionals are parameterized by using experimental or highly accurate *ab initio* data. The B3LYP (Becke, 3-parameter, Lee-Yang-Parr)[62,63] is one of the most well-known DFT and tested methods in computational chemistry. This functional[64] employs three empirical parameters[65,66]. Originally, it has been tested on 56 atomization energies, 42 ionization potentials, 8 proton affinities, and 10 total atomic energies of first and second-row systems and it was found that this functional fit experimental atomization energies with an impressively small average absolute deviation of 2.4 kcal/mol[67]. In terms of calculation time,

the B3LYP is generally faster than most of the post-Hartree-Fock methods and usually provides comparable results, which is especially hold for geometry.

The *ab initio* methods discussed so far provides accurate geometry, but to get more precise energy calculations results, higher-level methods such as CCSD, QCISD, CCSD(T), QCISD(T) are recommended. However, it has to be noted that using high level of theory methods costs a longer calculation time.

2.2.2 Basis set

A basis set is a collection of mathematical functions used to construct the quantum mechanical wave function of a molecular system. All of the previously mentioned electronic structure methods require a basis set to describe the electronic wave function. In principle, if the number of the mathematical functions used is high, the description of the electronic structure would be more accurate, and again, the drawback is the higher computing time. The minimal basis sets contain the minimal number of basis functions needed for each atom. The most common minimal basis set is STO-nG, where n is an integer. This n value represents the number of primitive Gaussian functions that comprise a single basis function. The STO-3G for example uses three Gaussian primitives per basis function, it is referred by "3G", "STO" stands for "Slater-Type Orbitals"[68]. However, the computation of the integrals is greatly simplified by the use of Gaussian-type orbitals (GTO)[69] for basis functions, however Gaussian functions are relatively fast to compute. The basis set can be made larger by increasing the number of basis functions per atom. Split-valence basis sets such as Pople basis sets[70], are defined as X-YZg. X is the number of Gaussian primitives comprising each core atomic orbital basis function. The Y and Z indicate that the valence orbitals are composed of two basis functions each, composed of a linear combination of Y and Z primitive Gaussian functions, respectively. In this case, the presence of two numbers after the hyphens implies that this basis set is a split-valence double-zeta basis set. Split-valence triple- and quadruple-zeta basis sets are denoted as X-YZWg, X-YZWVg, etc. There is one basis function for the core electrons and two or more for the valence. When the core orbital is made of 6 Gaussians and the valence is described by 2 orbitals (first is derived from 3 Gaussians and the second from 1) the basis set is called: 6-31G. Polarization can also be added to the non-hydrogen (d) and the hydrogen atoms as well (p)[71].

Ones of the most widely used basis sets are those developed by Dunning and coworkers[72] abbreviated as (aug-) cc-pV*N*Z, where the size of the basis grows with *N*. The term V*N*Z refers to "valence *X*-tuple zeta" where *N*=D,T,Q,5…(Double, Triple, Quadriple, etc.). The "cc-p",

stands for “correlation-consistent polarized” indicating that more functions with higher angular momentum quantum numbers are involved, and the “aug-” means “augmented” and indicates the inclusion of diffuse functions. For period-3 atoms (Al-Ar), additional functions have turned out to be necessary; these are the cc-pV(N+d)Z basis sets.

2.3 Composite methods

Quantum chemical composite methods are a combination of several computational chemistry methods aimed at achieving high accuracy at a relatively low cost. They are also called thermochemical recipes and are commonly used to calculate thermodynamic properties of molecules in chemical reactions. Various families of these exist, including Gaussian (Gn)73, Complete Basis Sets methods (CBS)74, and also Weizmann (Wn)75. The W1 protocol is based on the B3LYP/cc-pV(T+d)Z method63 for geometry optimization76 and frequency calculation77, followed by coupled cluster calculations for the thermochemical parameters. This protocol will be used for the calculations done in this work

2.4 Solvent model

To compute reactions in an aqueous phase, the solvent effect on the reaction has to be taken into account. To do this, different solvent models can be used, and are usually described as implicit or explicit solvent models.

2.4.1 Implicit models

Implicit or continuum solvent models, are models based on the assumption that explicit solvent molecules can be replaced by a homogeneous polarizable medium as long as this medium yield results that are an acceptable degree of accuracy to the explicit solventn[78]. Generally, for implicit solvents, the solute is encapsulated in a cavity containing the solute within the solvent continuum. The dielectric constant of the mimicked solvent is the value responsible for defining the degree of polarizability of the solvent continuum. The charge distribution of the solute affects the continuous dielectric field at the interface and polarizes the surrounding medium, which then causes a change in the polarization of the solute. This defines the solvation potential, the response to the change in polarization induced by the solvent on the solute.

Several standard models exist and have all been used successfully in a number of situations. The Polarizable Continuum Model (PCM) is a commonly used implicit model and has seeded the birth of several variants[79].

2.4.2 Explicit models

Explicit solvent models treat the solvent molecules explicitly. This is a more realistic picture since there are direct, specific solvent interactions with the solute, in contrast to continuum models. These models generally occur in the application of molecular mechanics (MM) and molecular dynamics (MD).

2.5 Potential energy surface and reaction mechanism

A potential energy surface (PES) is a multi-dimensional mathematical representation of the energy variations happening during chemical reactions as a function of the configuration of the system.

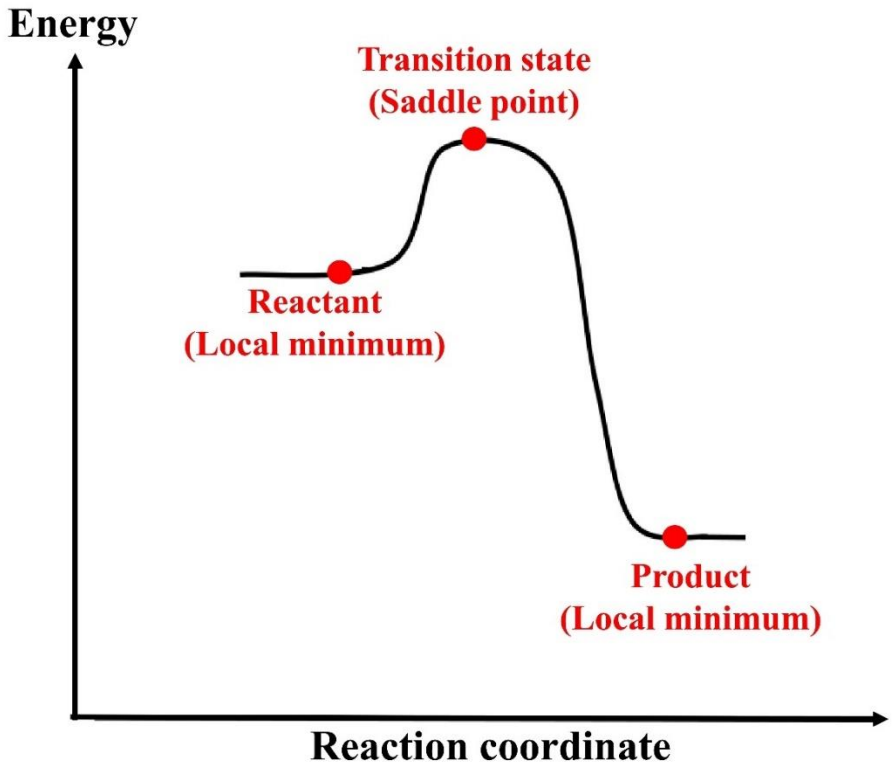

Figure 13: Schematic representation of a 2D potential energy surface (PES).

In order to explore the steps of a reaction, i.e. the reaction mechanism, the initial reactants, the final products and the intermediate structures as well as the transition structures of a reaction pathway have to be determined (**Figure 13**). The PES diagram helps to visualize and compare the energy levels of the reactants, products, intermediates, as well as the energy barriers, and therefore distinguish the rate limiting steps and select the preferable pathways for the reaction. Geometry optimization generally attempt to locate minima on the potential energy surface, thereby identifying equilibrium structures of molecules in the system. Optimizations can also

locate transition state structures in the system. At both minima and saddle points, the first derivative of the energy with respect to all internal coordinates, known as the gradient, is zero. The structure at these stationary points may correspond to a minimum (either a reactant, reaction intermediate, or product) or to a saddle point, which is a minimum in one direction of the PES, and a maximum in one or more directions. First-order saddle points, which are a maximum in one direction and a minimum in all other directions, correspond to transition-state structures. This is determined by calculating the Hess matrix.

The first critical step that has to be made before any quantum chemical calculation is to build the initial structure which is close enough to the sought structure. The Gaussian 09 program[80] can determine optimized structures by changing the structural parameters and calculating the corresponding electronic energy and the nuclei-nuclei repulsion energy (their sum is the so-called total energy, E_{tot}) at the selected level of theory. The minimum energy structure is formed when all the convergence criteria are fulfilled. The optimization is done as the following, in each iteration of the geometry optimization, the maximum remaining force on an atom in the system as well as the average mass weighted force constant on all atoms together has to be checked, and their values must be smaller than the corresponding threshold value. Furthermore, two other criteria also have to converge (maximum displacements). The maximum structural change of one coordinate, and the average standard deviation (RMS) change over all structural parameters in the last two iterations. Once the values of all four criteria fall below the given threshold, the optimization is considered as complete. After optimization, frequency calculation at the optimized geometry of the predicted structure will confirm if that is in fact a minimum. Frequency calculations consider the nuclear vibration in the molecular systems as if they are in their equilibrium states. If the geometry is optimized into a minimum, the gradient is zero, and the force constant matrix determines the behavior of the system under small displacements.

The Gaussian 09 program package[80] was used to carry out the calculations described this work. Detailed mechanisms of the uncatalyzed CO_2 hydrogenation to achieve methanol in gas phase and in aqueous phase have been studied thermodynamically. After that, a catalyzed-like aqueous phase mechanism has also been described. The W1 protocol has been chosen to carry out all the calculations

2.6 Gas phase calculations

As the hydrogenation of carbon dioxide is a complicated process, various computational chemical tools (combinatorial chemistry[83] in combination with *ab initio* calculations followed by thermodynamic calculations using the W1 protocol) have been applied to understand the mechanistic details of the process. The molecular complexes were generated using the MOLGEN 5.0 software[84], and after that, all the generated structures were optimized.

2.6.1 Structure generation

If the nuclei and chemical bonds are considered as the nodes and the edges of a graph, respectively, the enumeration of all the molecules corresponding to our stoichiometry (CH_8O_2) from a graph theory[84] is be possible. A certain number of atoms with a limited number of different valences defines the number of constitutional isomers[85]. All possible stoichiometric isomers of CH_8O_2 are generated by allowing carbon to form 2 or 4 chemical bonds, while hydrogen and oxygen to form 1 and 2 chemical bonds, respectively. This graphical representation is extended to three dimensions by the means of the atom-type specific geometric parameter set obtained from the MM2 force field. This procedure yielded 27 three-dimensional molecular configurations of the CH_8O_2 formula using the Molgen 5.0 program[84]. These configurations are used as initial structures in the search for local minima on the multidimensional potential energy surface for all the species.

2.6.2 Quantum chemical calculations

Additionally, the W1BD composite method[75] was selected to calculate all of the species. The W1BD method is the Brückner doubles variation of the Weizmann-1 (W1)[86] calculation scheme. The BD algorithm, which is employed in this method, involves macro iterations to update the orbitals[75]. A network of geometrically optimized reactants, intermediates and products for the uncatalyzed hydrogenation of CO_2 to methanol and methane is proposed. Beside the stable species, all transition states (TS) were also characterized by using the W1BD lmethod. The transitions states have also been verified by normal mode analysis and IRC (Internal Reaction Coordinates)[87] calculations. All the calculations were carried out with the Gaussian 09 software package[80]. The overall potential energy surface (PES) was constructed from the individual relative energies of the obtained structures.

2.7 Aqueous phase calculations

2.7.1 Uncatalyzed mechanism

A reaction mechanism involving a water molecule and protonation steps has been constructed starting with an initial reactant mixture of CO_2, $3H_2$, H_2O, and H_3O^+. All the thermodynamic properties of the involved species and transition states have been computed at standard conditions by using the Gaussian 09 program package[80]. The Potential Energy Surface (PES) of the studied reaction has been analyzed and the important points (minima, TS, etc.) have been located. IRC calculations have been used to verify the transition states are located between the corresponding minima. Initially, the calculations have been carried out by using the B3LYP density functional theory (DFT) method[88,89] in combination with the 6-31G(d) basis set[69]. To further improve the accuracy of the analysis, the structures have been recalculated by using the W1U (Unrestricted Weizmann-1) composite method[75,86,90]. In our previous work (gas phase)[91], the W1BD[75] protocol was applied for gas phase calculations, but it is not applicable in this case. The BD algorithm is not compatible with the SCRF implicit solvation model[92]. Thus, the W1U method was selected instead and the solvent effect have been mimicked by using the conductor-like polarizable continuum model (CPCM)[93,94]. To validate the choice of W1U, it was compared to W1BD in gas phase calculations and they gave almost identical results within less than 1 kJ/mol deviation (see section **2.8.3**).

2.7.2 Catalyzed-like mechanism

In catalyzed hydrogenation reactions, the hydrogen molecule is first split into hydrogen atoms. Thus, the hydrogen addition reactions are replaced by atomic hydrogenations ($H^{\bullet}$). Using $CO_2+6H^{\bullet}+H_2O+H_3O^+$ as reactants, the thermodynamic properties of the intermediate species and transition states for the formation of have been computed at standard conditions using the Gaussian 09 program package[80]. The new reactions were first calculated using the B3LYP/6-31G(d) level of theory[69] to pre-locate the minimas and transition states of the of the system. The energies of the reactions were subsequently recalculated by using the W1U (Unrestricted Weizmann-1)[75,86,90] composite method for higher accuracy. Internal Reaction Coordinate (IRC)[87] calculations have been carried out to verify that the transition states are located between the corresponding minima. Relaxed energy scans have been carried out to verify the barrierless reactions. In one case, a rigid energy scan (discussed in section **3.3**) was performed by freezing an inter atomic angle to avoid some undesirable interactions. Since this reaction takes place in the aqueous phase, the solvent effect has been mimicked by using the conductor-like polarizable continuum model (CPCM)[93,94].

2.8 Methods validation

2.8.1 Gas phase

To estimate the accuracy of the theoretical level and to determine its appropriateness as a method for our system, the heat of formation of 10 optimized structures have been calculated using the Feller-Helgaker extrapolation procedure[81,82] and the W1BD composite method and compared to experimental values (**Table 3**). To achieve the results using the Feller-Helgaker extrapolation, all structures had to be geometrically optimized with the MP2/aug-cc-pVTZ level of theory[95,96]. Then, the outputs are submitted for single point calculations using the CCSD(T)[97] method combined with the cc-pVTZ, cc-pVQZ, and cc-pV5Z[72] basis sets.

Table 3: Heat of formation ($\Delta_f H^0$) of 10 optimized structures calculated by using the Feller-Helgaker (F.H.) extrapolation and the W1BD method and compared to experimental values from the literature. All values are in kJ/mol.

Species	$\Delta_f H^0$		Experiment	Ref.	$\Delta\Delta_f H^0$	
	F.H.	W1BD			F.H.	W1BD
HCOOH	-373.62	-381.11	-378.80	[98]	5.18	2.31
CO	-106.81	-110.17	-110.53	[99]	3.72	0.36
CH_2	430.42	428.76	428.80	[100]	1.62	0.04
CO_2	-388.14	-394.67	-393.51	[99]	5.37	1.16
H_2CO	-107.25	-110.59	-108.70	[98]	1.45	1.89
CH_3OH	-202.04	-205.11	-201.00	[98]	1.04	4.11
CH_4	-72.65	-76.43	-74.60	[98]	1.95	1.83
H_2O	-244.70	-244.31	-241.81	[101]	2.89	2.50
H_2O_2	-137.69	-134.38	-135.77	[101]	1.92	1.39
H_3COOH	-128.07	-130.50	-131.00	[102]	2.93	0.50
			Average		2.81 ± 1.53	1.61 ± 1.21
			Max. dev.		5.37	4.10

Both methods yield results are in good agreement with the experimental values. However, the average deviation as well as the maximum deviation are smaller in the case of the W1BD method. Thus, it was selected for further calculations.

2.8.2 Aqueous phase

In the aqueous-phase calculations, the unrestricted version of the W1 method (W1U) has been chosen. To estimate the accuracy of the level of theory used in this case, calculations have been carried out to study reaction enthalpies of a simple mechanism which is close to our system (converts CO_2 and hydrogen to methanol and methane, **Figure 14**). The results have been compared to experimental values (**Table 4**) by using the heat of formations of the species available in the literature[102].

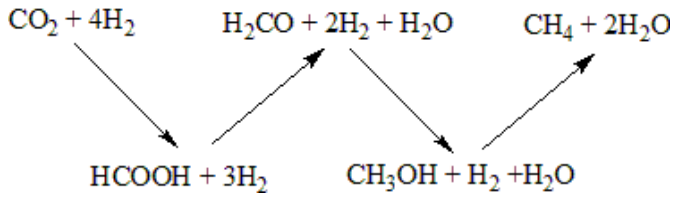

Figure 14: Reaction steps of CO_2 hydrogenation to methane.

The envisaged test reaction includes successive H_2 addition steps, where the formic acid, formaldehyde and methanol are formed, leading to the formation of methane (**Figure 14**).

Table 4: Comparison of the computed enthalpy changes (ΔH_r^o) of each molecule produced through elementary reaction steps and their respective experimental gas phase enthalpy of formation ($\Delta\Delta_f H^0_{exp}$) differences. The calculated and experimental values have also been compared and listed in the table (Calc-Exp).

	ΔH_r^o (kJ/mol) Calc	$\Delta\Delta_f H_{exp}^o$(kJ/mol) Exp	Abs. dev. (kJ/mol)
$CO_2 + 4H_2$	0.00	0.00	0.00
$HCOOH + 3H_2$	13.93	14.91	0.98
$H_2CO + 2H_2 + H_2O$	40.08	35.78	4.30
$H_3COH + H_2 + H_2O$	-53.78	-49.81	3.97
$CH_4 + 2\ H_2O$	-169.16	-165.02	4.14

The highest absolute deviation between the computed and the experimental values was obtained for the $H_2CO + 2H_2 + H_2O$ reaction and is equal to 4.30 kJ/mol. All in all, it can be considered that our computed results are precise and applicable to study CO_2 hydrogenation reactions.

2.8.3 Results comparability

In order to be able to compare the results calculated using two W1 sub-protocols (W1BD and W1U), we have to prove that they have very similar results for the same calculations (**Table 5**).

Table 5: Comparison of the computed absolute deviations of the results of the two arbitrarily chosen molecules formaldehyde and methanol using the W1BD and W1U protocols.

Energies (kJ/mol)	Abs. Dev. of the results from W1BD and W1U	
	Formaldehyde	**Methanol**
ZPE	0.000	0.000
Thermal Energy	0.000	0.000
Tot. Energy	0.985	0.396

The highest deviation between the two methods is less than 1 kJ/mol. Thus, it can be concluded that the W1U method is applicable and the two methods can be compared.

3 Results and Discussion

“The world is a book, and those who do not travel read only a page”

Saint Augustin

Born, lived, and died in Algeria

(354-430)

This chapter is a collection of the results of three major computational chemistry studies:
The first part of the results section is dedicated to the gas phase results. The results of the combinatorial chemistry calculations used to select the most stable molecular complexes identified the (CO_2+$4H_2$) reaction mixture will be shown. The selected molecules will be used to design a network for the uncatalyzed hydrogenation of carbon dioxide to methanol and methane. The results of the energetically studied network will be presented, and the efficiency of the most favorable pathway will be calculated.
After that, the aqueous phase results will be listed. It is a mechanistically studied water enhanced hydrogenation mechanism for CO_2 conversion to methanol. The efficiency of the preferred pathway will be calculated and compared to the gas phase results.
In the end, the results of the aqueous phase catalyzed-like study will be shown. This study has been made to mimic this special property of the solid catalysts to split the hydrogen molecules to hydrogen atoms. A catalyzed-like mechanism will be constructed and studied energetically, and the efficiency will be calculated taking into account the hydrogen bond dissociation energy.

3.1 Gas phase results

All the possible molecules and molecular complexes that can be described by the CH_8O_2 formula and involved in the gas phase uncatalyzed CO_2 hydrogenation to methanol and methane (*e.g.* CO_2 + $4H_2$, CH_4 + $2H_2O$) have been investigated[91]. By selecting the most stable intermediate molecules, a network of the hydrogenation process has been constructed. The thermodynamics of stable species and all the energy barriers were calculated using computational chemistry tools[103], and the most favorable pathway leading to methanol and methane has been selected. The structures have been generated by using the MOLGEN 5.0 software[84] and optimized by using the Gaussian 09[80] program package. the corresponding relative Gibbs free energy values were plotted against the relative entropies (**Figure 15**) to compare the stability of the species. Since the reactant mixture is CO_2 + $4H_2$, we have decided to consider it as a reference level.

The relative Gibbs free energy of every (X) structure will be calculated as follows:

$$\Delta G_r^o = \Delta G_{(X)} - \Delta G_{ref} \qquad (2)$$

The relative enthalpy and entropy were derived analogically.

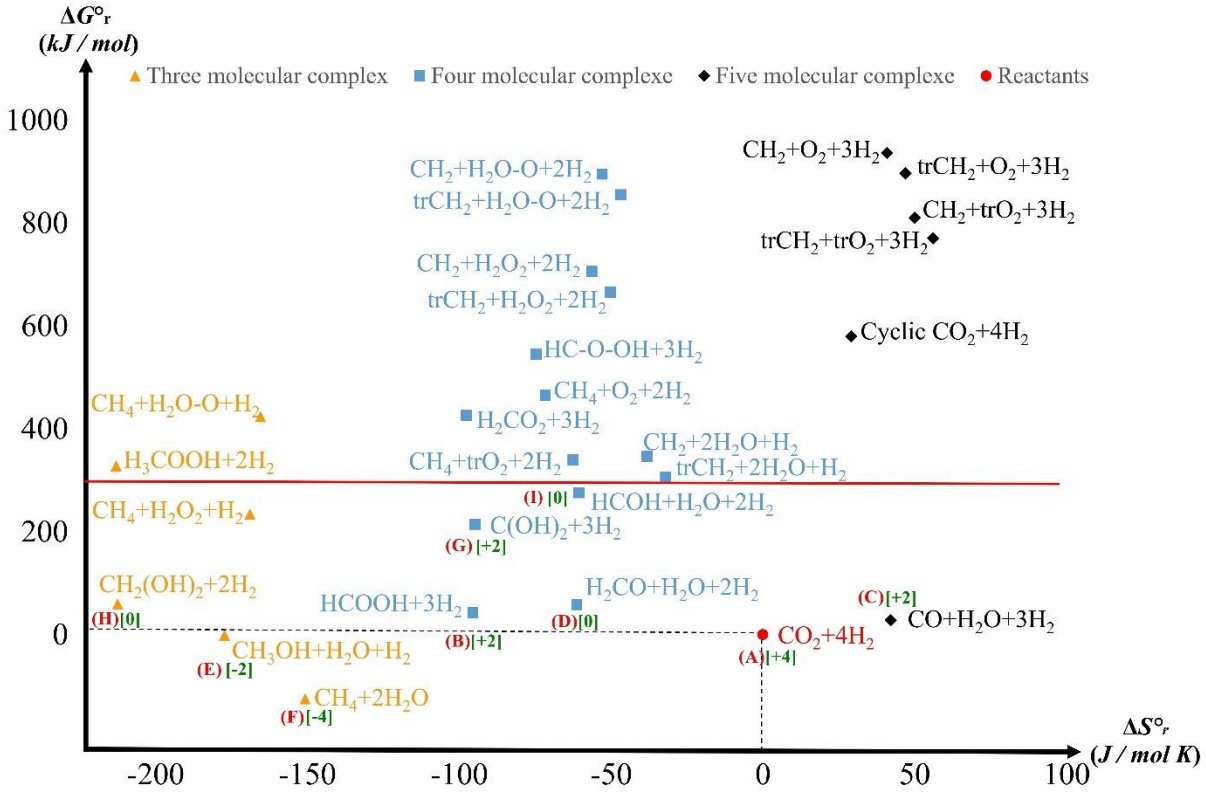

Figure 15: Thermodynamic properties of the stable molecules comprised of the CH_8O_2 formula which could be involved in CO_2 reduction. Relative Gibbs free energy (ΔG_r^o) and entropy (ΔS_r^o) were computed using the W1BD method for the molecular composition obtained by combinatorial tools. Molecules in the triplet electronic state are signed by tr. The red line defines the highest energy level of the stable section (>300 kJ/mol). The oxidation state of the most stable structures is shown in green. The energy of CO_2 + $4H_2$ species is considered as the reference level and is highlighted with a red dot.

Considering the number of molecular complexes generated by the CH_8O_2 formula (26 complexes), the **Figure 15** shows well-separated groups of species in a function of the entropy. The yellow triangles represent the three-, the blue squares the four-, while the black diamonds the five-membered complexes (**Table 6**). Only the methanol and methane complexes have lower free energy compared to the reference and both complexes have significantly lower entropy compared to the reference. This total entropy lowering could be hindered by the positive influence of the temperature on the equilibrium. We have considered the complexes having a relative Gibbs free energy lower than 300 kJ/mol as relatively stable.

Table 6: Thermodynamic properties of the molecular complexes generated using the CH_8O_2 stoichiometry calculated at the W1BD level of theory.

	Species	ΔG_r^o (kJ/mol)	ΔH_r^o (kJ/mol)	$\Delta S°$ (J/mol K)
5 Molecules	**CO+H₂O+3H₂**	40.27	27.70	42.15
	CH₂+O₂+3H₂	948.93	936.73	40.90
	trCH₂+O₂+3H₂	910.53	896.52	47.00
	CH₂+trO₂+3H₂	825.63	810.72	50.03
	trCH₂+trO₂+3H₂	787.24	770.51	56.12
	Cycle_CO₂+4H₂	588.46	579.78	29.11
4 Molecules	**HCOOH+3H₂**	13.65	42.14	-95.56
	H₂CO+H₂O+2H₂	39.94	58.22	-61.32
	C(OH)₂+3H₂	186.34	214.61	-94.84
	HCOH+H₂O+2H₂	257.86	275.93	-60.61
	HC-O-OH+3H₂	522.99	545.24	-74.62
	CH₂+H₂O₂+2H₂	689.22	706.02	-56.34
	trCH₂+H₂O₂+2H₂	650.83	665.81	-50.25
	CH₂+2H₂O+H₂	335.07	346.44	-38.15
	trCH₂+2H₂O+H₂	296.67	306.23	-32.05
	H₂CO₂+3H₂	396.79	425.92	-97.68
	CH₄+O₂+2H₂	443.82	465.19	-71.69
	CH₄+trO₂+2H₂	320.52	339.18	-62.57
	CH₂+H₂O-O+2H₂	879.74	895.52	-52.91
	trCH₂+H₂O-O+2H₂	841.35	855.31	-46.81
3 Molecules	**CH₃OH+H₂O+H₂**	-54.49	-1.62	-177.33
	CH₄+2H₂O	-170.04	-125.10	-150.74
	CH₂(OH)₂+2H₂	-3.47	59.90	-212.51
	H₃COOH+2H₂	264.34	327.85	-213.03
	CH₄+H₂O₂+H₂	184.11	234.48	-168.93
	CH₄+H₂O-O+H₂	374.64	423.98	-165.50

It is important to note that CO formation (third most stable complex) has an entropy increasing by 40 kJ/mol·K, therefore, it would be a preferred way to improve CO_2 reduction by increasing the temperature. This complex without water could be referred to as the classical syngas and can open different catalytic reduction pathways. Complexes of all other stable oxidation states of carbon can be found within a 60 kJ/mol relative Gibbs free energy range.

The structures were divided into three clusters:

- High energy cluster (above the red line; $\mathbf{\Delta G_r^o > 300\ kJ/mol}$).
- Energetically favoured cluster (below the reference; $\mathbf{\Delta G_r^o < 0\ kJ/mol}$).
- Energetically available cluster (between the red line and the reference, $\mathbf{0\ kJ/mol < \Delta G_r^o < 300\ kJ/mol}$).

To construct molecular networks that could lead to the desired product, we considered the molecules within the energetically favored and available clusters.

The [CH_4+H_2O_2+H_2] molecular complex was not included in the reaction network. Methane is already a part of the [CH_4+2H_2O] complex, which is energetically the lowest of all the clusters ΔG_r^o **[CH_4+2H_2O]** = -170.04 kJ/mol.

The proposed reaction network (**Figure 16**) summarizes various reaction pathways that lead to the formation of methanol and methane by considering the molecular complexes that have a relative Gibbs free energy less than 300 kJ/mol.

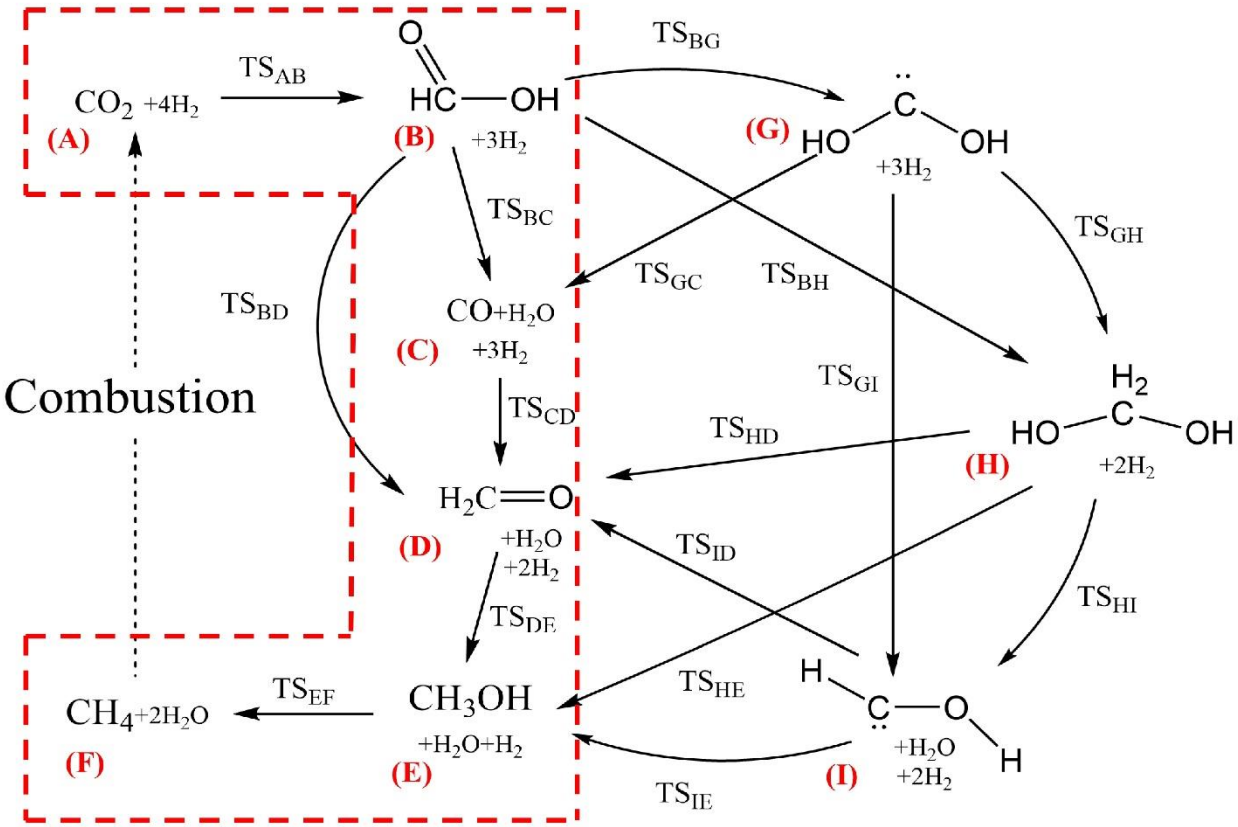

Figure 16: A network describing the formation of methanol and methane through CO_2 hydrogenation. Letters are assigned to each structure, and each transition state is labelled as TS followed by the letters referring to the reactant and then the product (*e.g.* TS_{AB}) respectively. The most energetically favourable route is highlighted with red lines.

The first intermediate of CO_2 hydrogenation is the formation of formic acid (**B**). Thereafter, the reaction pathway diverges into several possible routes:

a) **The ABDEF route:** three successive direct hydrogenations of formic acid (**B**) (**TS_{BD}, TS_{DE}, TS_{EF}** respectively) could lead to the formation of methane (**F**) through formaldehyde (**D**), and methanol (**E**) intermediates, along with the formation of two

water molecules. If the reaction **BD** can be replaced by two elementary reactions (**TS_{BC}, TS_{CD}**) then carbon monoxide (**C**) can be formed.

b) **The ABGHIE route:** a hydrogen shift in formic acid (**TS_{BG}**) could lead to (**G**) which is a relatively stable triplet state structure. From this point, methanediol $CH_2(OH)_2$ (**H**) can be achieved by H_2 addition. These two reaction steps can be replaced by a direct hydrogenation (**TS_{BH}**). After that, with a water elimination (**TS_{HI}**) followed by a hydrogenation, methanol is formed. A shortcut getting around the reactions (**TS_{HI}** and **TS_{IE}**) is also possible, with a hydrogenation and a water elimination occurring at the same time (**TS_{HE}**) and methanol can be reached.

c) The above described routes can also be connected as follows:
   - A water elimination from (**G**) could lead to CO (**C**) through **TS_{GC}**.
   - Formaldehyde can be reached by a water elimination from methanediol (**H**) and by a hydrogen shift in (**I**).

The classical combustion of methane can close the thermodynamic cycle.

The longest route to reach methanol and then methane is the following:

CO_2-**TS_{AB}**-HCOOH-**TS_{BG}**-$C(OH)_2$-**TS_{GH}**-$H_2C(OH)_2$-**TS_{HI}**-HCOH-**TS_{ID}**-H_2C=O-**TS_{DE}**-CH_3OH-**TS_{EF}**-CH_4. It contains 7 steps.

In contrast to that, the shortest route to reach methanol and then methane contains 4 steps only:

CO_2-**TS_{AB}**-HCOOH-**TS_{BD}**-H_2C=O-**TS_{DE}**-CH_3OH-**TS_{EF}**-CH_4.

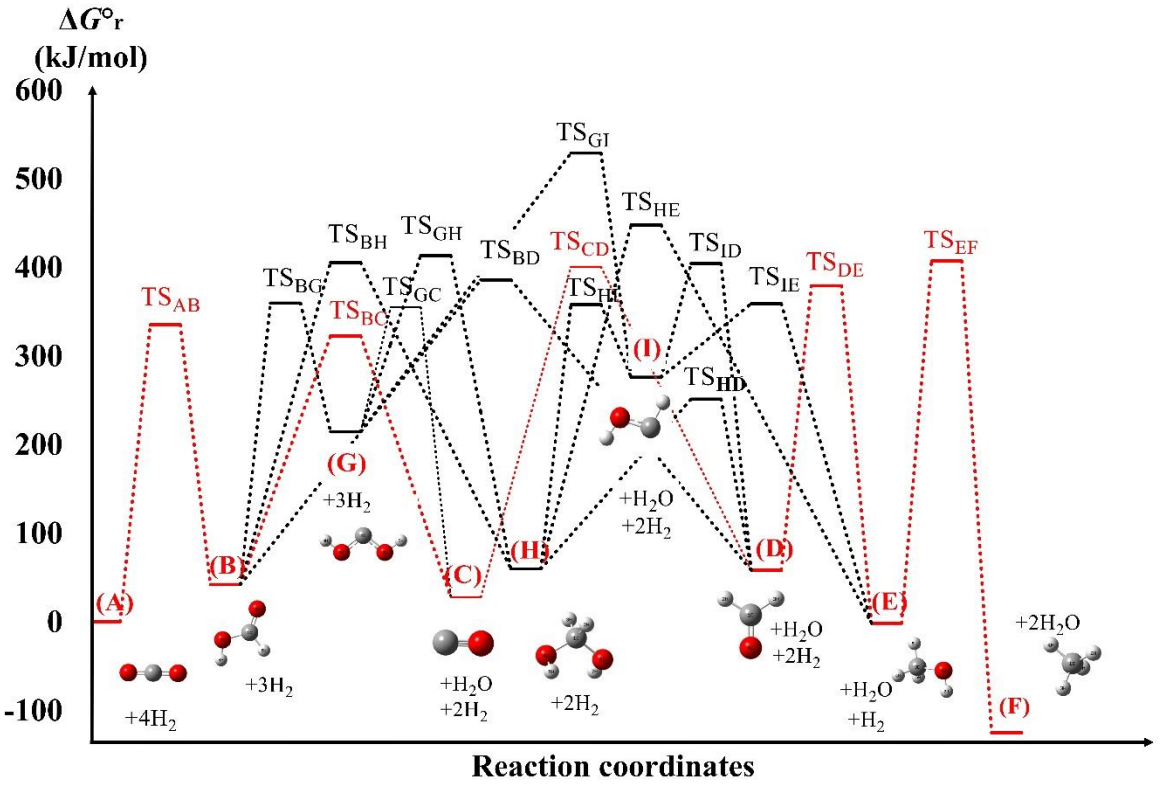

Figure 17: Gibbs free energy profile of the uncatalyzed hydrogenation of CO_2 to methanol and methane calculated at the W1BD level of theory plotted against the reaction coordinates with a highlighted energetically favoured route in red.

All Gibbs free energy values of the transition states are in the range of [250-530] kJ/mol (**Table 8**). The lowest energy reaction path leading to the products has been selected (**Figure 17**, red). The highest energy barrier, which corresponds to the rate limiting step ($\Delta G^{o}_{TS\_CD}$= 400.66 kJ/mol), is the energy needed to cross over all the barriers and reach methanol. In order to produce methane, another even higher barrier has to be overcome ($\Delta G^{o}_{TS\_EF}$ = 407.18 kJ/mol).

Thus, the most feasible reaction pathway for methanol and methane production is:
Carbon dioxide (**A**) – **TS_{AB}** – formic acid (**B**) – **TS_{BC}** – carbon monoxide (**C**) – **TS_{CD}** – formaldehyde (**D**) – **TS_{DE}** – methanol (**E**) – **TS_{EF}** – methane (**F**).

Another pathway which has to be mentioned, is the **ABHDEF**. This pathway involves the lowest transition state of the overall network (**TS_{HD}**= 251.20 kJ/mol). Unfortunately, the rate limiting step ($\Delta G^{o}_{TS\_BH}$= 405.60 kJ/mol) is slightly higher (4.94 kJ/mol) than the rate limiting step of the preferred pathway **ABCDEF**. Otherwise, this route would have been more preferable.

The CO (**C**) can be a key intermediate, as its formation can be influenced (slightly increased) with temperature. It allows a different entrance to the network, the classical syngas reaction[104].

Table 7: Thermodynamic properties (ΔH_r^o, ΔG_r^o in kJ/mol and S in J/mol.K) of the stable structures and the transition states involved in the reaction network calculated at the W1BD level of theory. The highlighted red values belong to the preferred pathway of the mechanism.

Code	Particules	ΔG_r^o	ΔH_r^o	S
		kJ/mol		J/mol K
A	CO_2+4H_2	0	0	734.73
B	$HCOOH+3H_2$	42.14	13.65	639.16
C	$CO+H_2O+3H_2$	27.7	40.27	776.88
D	$H_2CO+H_2O+2H_2$	58.22	39.94	673.41
E	$CH_3OH+H_2O+H_2$	-1.62	-54.49	557.40
F	CH_4+2H_2O	-125.1	-170.04	583.99
G	$C(OH)_2+3H2$	214.61	186.34	639.89
H	$CH_2(OH)_2+2H_2$	59.9	-3.47	522.21
I	$HCOH+H_2O+2H_2$	275.93	257.86	674.11
TS_{AB}	A → B	334.82	306.20	638.74
TS_{BC}	B → C	322.64	297.84	651.54
TS_{CD}	C → D	400.66	383.07	675.73
TS_{DE}	D → E	379.21	324.86	552.42
TS_{EF}	E → F	407.18	321.41	447.05
TS_{BH}	B → H	405.60	341.09	518.38
TS_{BG}	B → G	359.65	331.98	641.89
TS_{GH}	G → H	413.22	350.92	525.75
TS_{HD}	H → D	251.20	186.88	519.00
TS_{HI}	H → I	357.97	297.89	533.21
TS_{ID}	I → D	404.19	386.36	674.92
TS_{IE}	I → E	359.06	305.89	556.41
TS_{HE}	H → E	447.74	353.81	419.67
TS_{GI}	G → I	529.02	468.55	531.92
TS_{BD}	B → D	385.91	322.70	522.72
TS_{GC}	G → C	355.00	327.66	643.04

The thermodynamic properties of the generated structures are divided into two sections in **Table 7**. The first part shows the properties of the stable intermediate molecular complexes involved in the network. The second part contains the activation Gibbs free energy, enthalpies as well as the absolute entropy of the transition states ($TS_{\alpha\beta}$), were α and β refers to the reactants and the products.

Storing energy would be possible only in exothermic reactions. In other words, it can happen only in the case of products having a negative reaction enthalpy. Although the methanediol (**H**) corresponds to a local minimum in the potential energy surface (**Figure 17**) with a negative relative enthalpy ($\boldsymbol{\Delta H^{o}_{CH2(OH)2}}$), it is a non-isolable product and almost thermoneutral. Thus, only two products are available for energy storage: methanol (**E**) and methane (**F**), with a relative enthalpy equal to -55 and -170 kJ/mol, respectively.

The CO_2 reduction can be achieved in different routes to form (**E)** and (**F)** (**Figure 16, Figure 17**). To store energy, the reactants should reach the highest energy point of the most energy efficient route. This is corresponding to the highest activation energy of the reaction path $\Delta H_{\mathrm{TS}}^{\mathrm{max}}$; and the system needs to achieve this energy to reach the product site. It can be assumed, that the theoretical efficiency of the energy storage can be estimated based on the computed thermodynamic functions. The theoretical efficiency can be defined by the ratio of the stored enthalpy $|\Delta H_{\mathrm{r}}^{\mathrm{o}}|$ and the invested enthalpy ($\Delta H_{\mathrm{TS}}^{\mathrm{max}}$), the highest enthalpy of the corresponding reaction path:

$$\eta = \frac{|\Delta H_{\mathrm{r}}^{\mathrm{o}}|}{\Delta H_{\mathrm{TS}}^{\mathrm{max}}} \qquad (3)$$

It can be concluded that the theoretical efficiencies of methanol **(E)** and methane (**F)** formation are $\boldsymbol{\eta_{(E)}} = 14.4$ % and $\boldsymbol{\eta_{(F)}} = 44.4$ %, respectively ($\Delta H_{\mathrm{TS}}^{\mathrm{max}}$ = ΔH(**TS$_{CD}$**) in both cases).

After analyzing the available results, it is obvious that in order to increase the efficiency of the energy storage, catalytic reactions are needed. Nevertheless, we have noticed a special molecule appearing as a constituent of several intermediate molecular complexes. This molecule is water (H_2O). As a consequence, since the hydrated version of CO_2 is the well-known carbonic acid ($CO(OH)_2$), the effect of a water molecule and protonation reactions on the reaction mechanism has been studied.

3.2 Aqueous phase results

In the gas phase network, the first and only elementary reaction was a hydrogenation, and the relative Gibbs free energy was quite high ($\Delta G^{o}_{TS\_AB}$= 334.82 kJ/mol). In the aqueous phase network, to avoid some of the hydrogenation, hydration and protonation steps have been included. The mechanism has been compared energetically with the previously studied gas phase process.

A newly designed CO_2 – methanol conversion mechanism is presented here[105], which involves several intermediates and transition states and applies $3H_2$, H_2O and H_3O^+ as additional reactants.

The reaction pathways leading to methanol are starting either with a hydration or a protonation step (**Figure 18**).

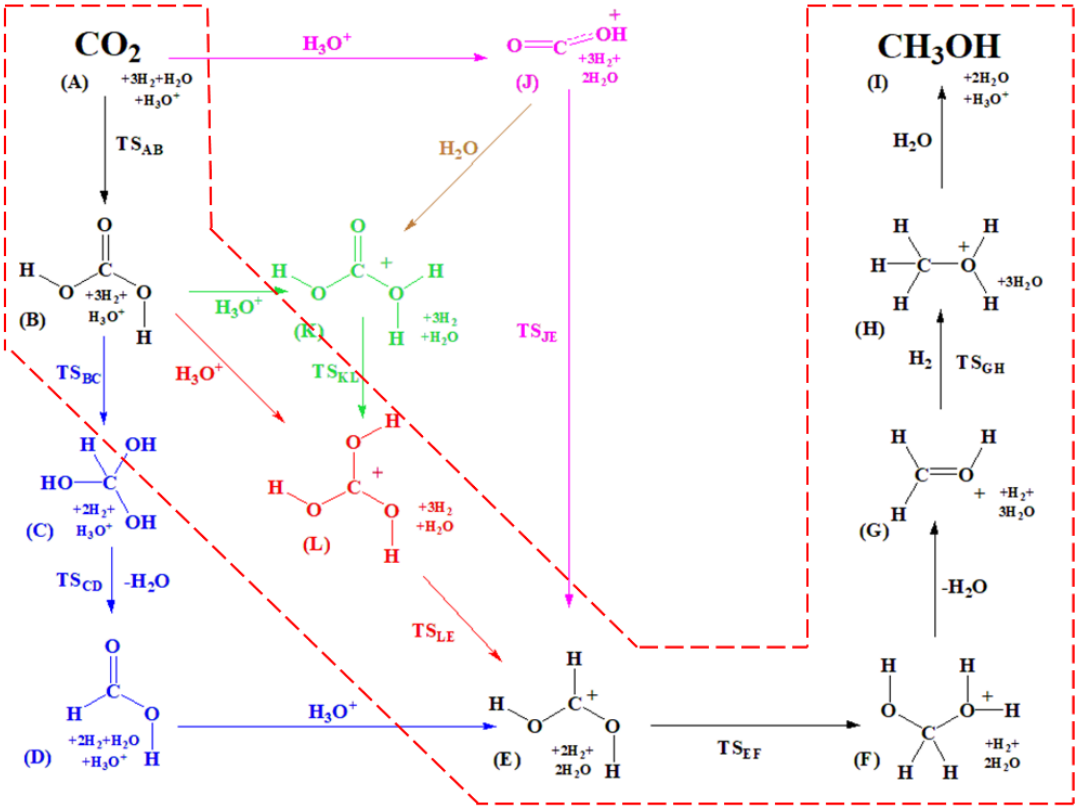

Figure 18: Reaction pathways of the envisaged water enhanced CO_2 – methanol conversion. Letters are assigned to every structure, and each transition state is named as TS followed respectively with the letter referring to the reactant and then the product (*e.g.* TS_{AB}). The preferred pathway is highlighted by dashed lines.

As a first step CO_2 (**A**) can be either hydrated to form carbonic acid (**B**), or protonated (**J**). The center element of the mechanism is the protonation of formic acid (**DE**). To reach this point, four alternative pathways can be followed:

a) The ABCDE route (blue): by the hydration of CO_2 (**A**) carbonic acid (**B**) will form (there are three conformations, the one considered here is higher in energy by 3.14 kJ/mol than the most stable conformation). This will be hydrogenated to reach methanetriol (**C**) which could go further towards formic acid (**D**) by a water elimination (**TS_{CD}**). Then, formic acid can be protonated to form (**E**).

b) The ABLE route (red): **(L)** can be achieved by the protonation of carbonic acid (**B**) which is the product of CO_2 hydration. The hydrogenation of **(L)** will lead directly through **(TS_{LE})** to the protonated formic acid **(E)** and the formation of an extra water molecule.

c) The AJE route (pink): The protonation of CO_2 followed by a hydrogenation **(TS_{JE})** leads directly to the protonated formic acid **(E)** through only two elementary steps.

d) **The AJKLE route** (green): In this route additional elementary steps and one intermediate molecule links the *red* and the *pink* routes mentioned above. The molecule (**K**) is a protonated carbonic acid, which can be formed through a hydration of the protonated carbon dioxide (**JK**) or by the protonation of carbonic acid (**BK**). Then, a hydrogen shift could occur (**TS_{KL}**) to produce (**L**).

Then, the protonated formic acid (**E**) is hydrogenated to form (**F**), from where a water elimination will lead to (**G**), which is a protonated formaldehyde. After this point, another hydrogenation (**TS_{GH}**) will occur to reach the protonated methanol (**H**) and the final step will be the release of the proton to a water molecule forming methanol (**I**) and hydronium ion.

The thermodynamic properties of the pathways have been computed (**Table 9**) and compared (**Figure 19**). $CO_2 + 3H_2 + H_2O + H_3O^+$ was selected as a reference to compute the relative thermodynamic properties of the individual steps (*e.g.* $\Delta G_r^o = G_{(X)} - G_{ref}$, where $G_{(X)}$ and G_{ref} are the Gibbs free energy of structure X and the reference species, respectively).

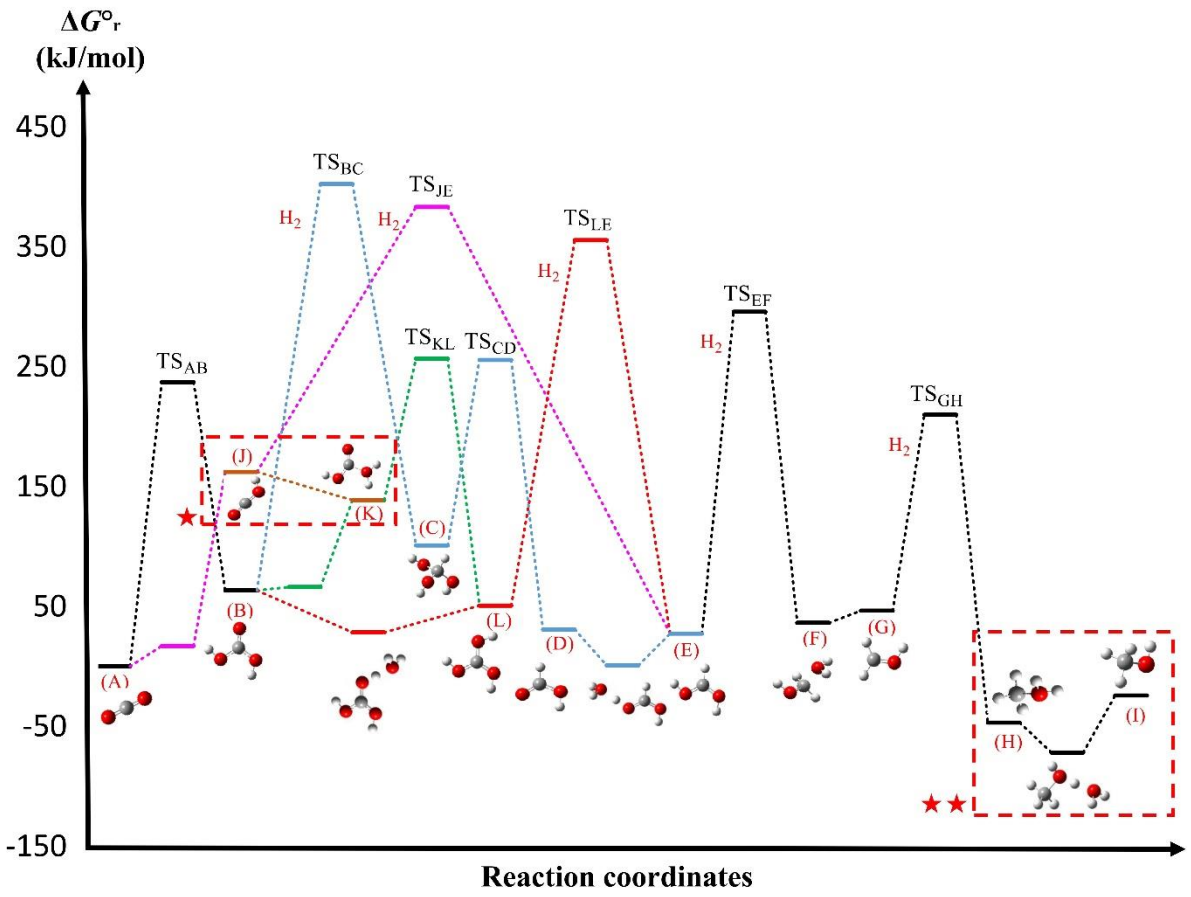

Figure 19: Gibbs free energy change (ΔG_r^o, kJ/mol) of the water enhanced conversion of CO_2 to methanol calculated at the W1U level of theory combined with the SCRF solvent model. The transition states are identified as TS followed by the reactant and the product, where the hydrogenation steps are highlighted with the (H_2) sign close to the barrier. (**B**), (**K**), (**E**) and (**L**) could have more than one conformer. *Morse potential - barrierless elementary reaction step **JK**. **Double Morse potential - barrierless elementary reaction step **HI**.

The mechanism can be divided into two parts: **[A-E]** and **[E-I]** (**Figure 19**). In the case of **[A-E]** the conversion of CO_2 (**A**) to protonated formic acid (**E**) occurs through several different pathways, whereas **[E-I]** is one single route where (**E**) will be converted to methanol (**I**) after 4 consecutive reaction steps.

In the **[A-E]** part of the mechanism, all the routes starts with a hydration of CO_2 (**A**) to carbonic acid (**B**), except for the *pink* pathway which goes directly from CO_2 (**A**) through a protonation followed by a hydrogenation to the protonated formic acid (**E**) with one single barrier ($\mathbf{\Delta G^o_{TS\_JE}}$ = 383.18 kJ/mol) which is the second highest energy barrier in the system. The *blue* pathway shows the possibility to reach (**E**) through three reaction steps, within which there are two transition states (TS) and one of which ($\mathbf{TS_{BC}}$) corresponds to the highest barrier height in the system with a value of 402.34 kJ/mol. The other two steps are ($\mathbf{TS_{CD}}$) ($\mathbf{\Delta G^o_{TS\_CD}}$= 255.58 kJ/mol) and (**DE**) which is a barrierless reaction step. Through the *red*

pathway, the protonated formic acid (**E**) can be reached from carbonic acid with only two reaction steps where one is a barrierless process (**BL**) while the other is a hydrogenation ($\Delta G^{o}_{TS\_LE}$= 355.52 kJ/mol). The hydrogenation (TS_{LE}) has the lowest energy barrier in the **[A-E]** section, and which makes this part of the preferred pathway. The overall preferred pathway is **[A-TS_{AB}-B-BL-L-TS_{LE}-E-TS_{EF}-F-G-TS_{GH}-H-HI-I]**. It is possible to link the *pink* and *red* pathways through the hydration reaction (**JK**) highlighted with the frame (*, **Figure 19**), followed by the hydrogen shift ($\Delta G^{o}_{TS\_KL}$= 256.78 kJ/mol) which is a part of the *green* reaction channel.

The two highlighted steps (**JK**) (*) and (**HI**) (**) are representing the two types of barrierless reactions (Morse potential) in the system (**Figure 19**). All the possible pathways involve protonation steps. It is important to note that, in these cases, the reaction is barrierless and goes through a minimum instead of a transition state, and these are double Morse potentials (association + dissociation). (**HI)** (**, **Figure 20**) was used as an example to describe these cases (**AJ, BK, BL, DE** and **HI**). The second type of barrierless step is a simple Morse potential reaction of a (de)hydration, where (**JK**) (*, **Figure 20**) was used as an example. This type can also be observed in the reaction **FG**.

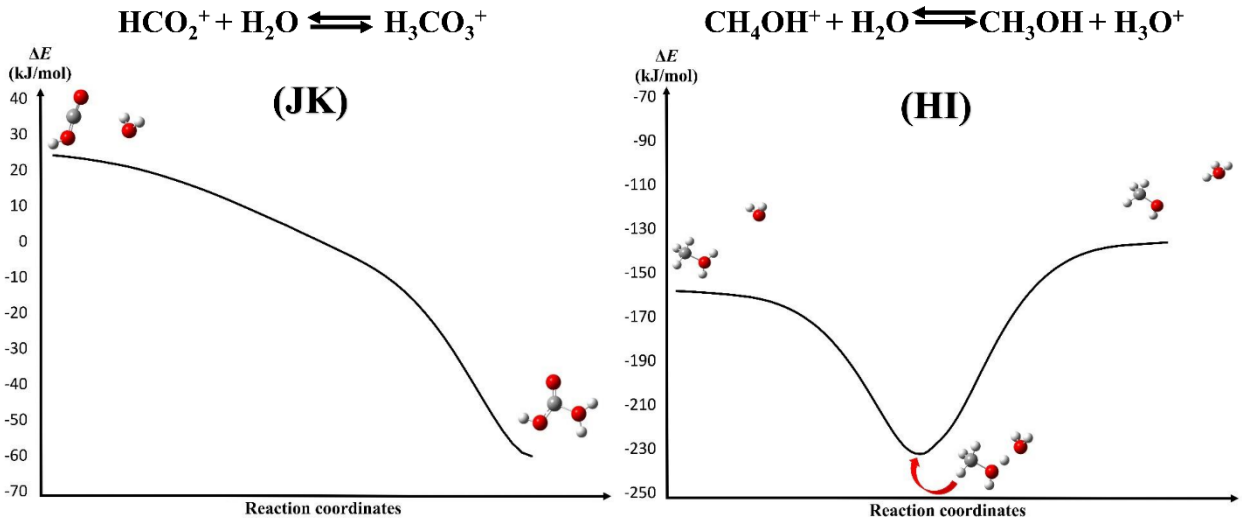

Figure 20: Total energy change (ΔE_{tot}) of the two types of barrierless reactions (**JK**) (Morse potential, hydration) and (**HI**) (Double Morse potential, protonation). Calculated at W1U level of theory combined with the SCRF solvent model.

The relative total energy change of the reaction (**HI**) (**Figure 20**, right panel) has a shape of a parabola with a plateau at each extremity. The beginning of the reaction is at the first plateau, where the water molecule and the protonated methanol form a complex (protonated methanol-water). After this point, the total energy decreases and reach a minimum (first Morse potential),

where the proton belongs to both methanol and water. Then, the energy increases to advance to another plateau (second Morse potential), where the products are located. Thus, the product is formed (methanol + H_3O^+) without going through an energy barrier.

In case of (**JK**) (**Figure 20**, left panel), the total energy decreases from the reactant energy level ($H_3COH_2^+$+H_2O) directly to the energy level of the products (H_3COH+H_3O^+) without going through an energy barrier.

Since the barrierless reaction (**DE**) is the second energetically lowest reaction of the system, it has also been studied through a flexible scan (**Figure 21**).

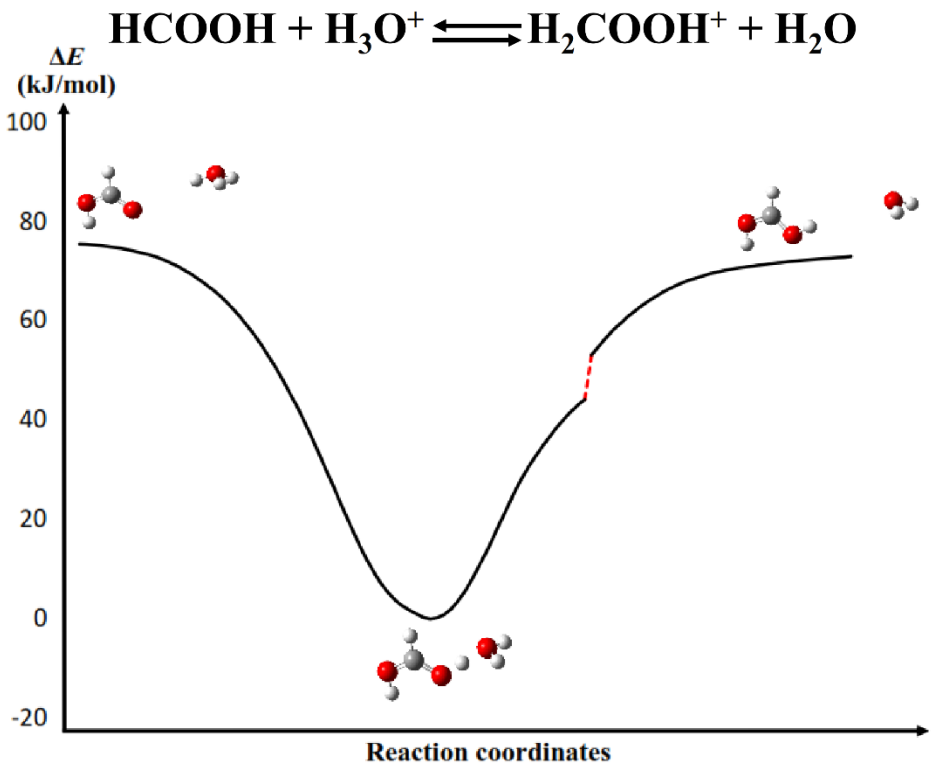

Figure 21: Total energy change (ΔE_{tot}) of the (**DE**) reaction step (double Morse potential). Calculated at W1U level of theory combined with the SCRF solvent model.

(**DE**) is a barrierless process, which is similar to (**HI**) discussed above. The reaction decreases to a local minimum where the total energy change is close to 0 kJ/mol, as well as the relative Gibbs energy (see ΔG_{DE}^{o} at the **Table 8**).

Table 8: Thermodynamic properties (ΔH_r^o, ΔG_r^o in kJ/mol and S in J/mol.K) of carbon dioxide – methanol conversion reaction mechanism calculated at the W1U level of theory combined with the SCRF solvent model. The transition states of each elementary reaction steps are named as TS followed with the letter of the reactant and then the product (*e.g.* **TS_{AB}**). The barrierless reactions are noted by giving a letter of the reactant followed by the product (*e.g.* **AJ**). The structures corresponding to the preferred pathway are highlighted in red.

Code	Particules	ΔH_r^o	ΔG_r^o	S
		kJ/mol		J/mol*K
A	CO_2	0.00	0.00	213.78
B	H_2CO_3	23.96	63.41	270.16
C	$HC(OH)_3$	28.15	100.93	288.63
D	HCOOH	2.30	30.80	248.48
E	$HCOOH_2^+$	-4.47	27.38	250.68
F	H_2O-H_2COH^+	-28.17	36.42	271.12
G	H_2COH^+	25.23	46.46	227.86
H	$H_3COH_2^+$	-101.81	-46.78	244.74
I	H_3COH	-77.06	-24.24	238.71
J	HCO_2^+	166.11	162.31	239.96
K	$H_3CO_3^+$	98.83	138.67	282.28
L	$C(OH)_3^+$	7.97	50.75	272.44
TS_{AB}	A → B	270.25	237.28	270.25
TS_{BC}	B → C	282.42	402.34	282.42
TS_{CD}	C → D	282.31	255.58	282.31
TS_{EF}	E → F	263.21	295.83	263.21
TS_{GH}	G → H	238.87	209.81	238.87
TS_{JE}	J → E	256.89	383.18	256.89
TS_{KL}	K → L	271.27	256.78	271.27
TS_{LE}	L → E	284.66	355.52	284.66
AJ	A-H_3O^+	-13.29	17.08	314.03
BK	B-H_3O^+	-9.17	65.54	354.05
BL	B-H_3O^+	-49.12	28.49	344.31
DE	D-H_3O^+	-66.50	0.97	319.88
HI	H-H_2O	-163.16	-71.79	311.58

At this point, the protonated formic acid is forming a molecular complex with a water molecule, and the energy increases with the increasing distance between the water molecule and the protonated formic acid. The red dashed part of the graphic represents an internal conformational change, the oxygen atom of the water molecule got an interaction with the second closest hydrogen from the protonated formic acid while the distance between the two molecules was increasing during the flexible scan.

The highest energy barriers of the water-mediated reaction network are $\Delta G^{o}_{TS\_BC}$= 402.34 kJ/mol, $\Delta G^{o}_{TS\_JE}$= 383.18 kJ/mol, $\Delta G^{o}_{TS\_LE}$= 355.52 kJ/mol and $\Delta G^{o}_{TS\_EF}$= 295.83 kJ/mol (**Table 9**), and all of the corresponding reaction steps are hydrogenations (H_2 molecule addition). Surprisingly, the last hydrogenation reaction step ($\Delta G^{o}_{TS\_GH}$= 209.81 kJ/mol) is in the range and even lower, than the other processes such as hydrations (*e.g.* $\Delta G^{o}_{TS\_AB}$= 237.28 kJ/mol), dehydrations (*e.g.* $\Delta G^{o}_{TS\_CD}$= 255.58 kJ/mol) and hydrogen shifts (*e.g.* $\Delta G^{o}_{TS\_KL}$= 256.78kJ/mol).

Exothermic reactions are necessary to be involved in energy storage applications, ($\Delta H°_r<0$). Although the relative enthalpy values of $HCOOH_2^+$, H_2O-H_2COH^+ and $H_3COH_2^+$ are negative (**Table 9**), these products are non-isolable, and thus, the only remaining option for energy storage will be methanol (ΔH^{o}_{H3COH} = -77.06 kJ/mol**)** in the system studied. Comparing this value to the amount of heat of the highest energy barrier (ΔH_{H3COH}= 284.66 kJ/mol) allow us to determine the theoretical efficiency of methanol formation in the mechanism. It corresponds to the ratio of the stored enthalpy $|\Delta H_r^o|$ and the invested enthalpy (the highest activation energy of the reaction path ΔH_{TS}^{max}) (**Equation (3)**).

The two preferred pathways of CO_2 conversion to methanol in gas phase (section **3.1**)[91] and aqueous phase[105] have been compared (**Table 9**). It has to be emphasized that the aqueous phase pathway involves some ionic and barrierless reactions, while the gas phase pathway doesn't. In the best aqueous phase pathway, there is only one energy barrier higher than 300 kJ/mol $\Delta G^{o}_{TS\_LE}$= 355.52 kJ/mol, unlike in the case of gas phase, where all the barriers are > 300 kJ/mol. The rate of the recovered energy from what has to be invested in the uncatalyzed methanol formation from CO_2 hydrogenation in gas phase and aqueous phase has also been provided, and in the case of the aqueous phase mechanism the efficiency is 27.1%, which is almost two times higher than in the gas phase (14.4%).

Table 9: The comparison of the preferred carbon dioxide-methanol conversion pathways in gas and aqueous phase.

	Gas phase[91]	**Aqueuse phase**
Barrierless reactions	No	Yes
Ionic reactions	No	Yes
Number of barriers >300 kJ/mol	All (4)	One
Highest energy barrier (kJ/mol)	400.66	355.52
Efficiency (η)	14.4%	27.1%

According to the results mentioned so far, the hydrogenation reaction barriers are in both of the gas phase and the aqueous phase mechanisms are higher than the average energy level of the rest of the elementary reactions. The challenge would be then to find alternative reactions to reduce the hydrogenation barriers. This can be done by adding the appropriate catalyst to the reaction which will reduce the hydrogenation barriers and alter the number of elementary steps. By considering a homogeneous process, there is no obvious choice for the catalyst to speed up the reaction by lowering the hydrogenation barriers. In the case of a heterogeneous process, metal based catalysts such as Cu/ZnO or nickel could be an adequate choice as they are already tested before[106,107]. However, in a catalytic system, hydrogen molecules (H_2) are split into hydrogen atoms ($H^{\bullet}$), and to study the process at the molecular level, the reaction mechanism should be altered accordingly.

3.3 Catalyzed-like aqueous phase mechanism for CO_2 conversion to methanol

The heterogeneous catalytic process of carbon dioxide hydrogenation will involve a bond breaking step within which hydrogen molecules will split into hydrogen atoms. The possibility of hydrogen bond dissociation occurring in the adsorption process of the H_2 molecule on the surface of a catalyst is discussed in several works in the literature[108,109]. In this mechanism, hydrogen atoms would be adsorbed and ready to react at the surface of the catalyst. Thus, the hydrogen addition reactions will be then replaced by atomic hydrogenations ($H^{\bullet}$). By studying such a system, new insights into the catalytic CO_2 conversion can be achieved, which can be applicable in catalyst design and development.

It is also worth mentioning water electrolyzers[110,111], where hydrogen atoms and ions might also be observed in the reaction media. This relatively new technology is designed to create electrolysis cells capable of realizing an electrolytic reduction of CO_2 to other carbon chemicals (CO, HCOOH, CH_3OH, and CH_4) using the hydrogen generated from the water electrolysis (**Figure 22**).

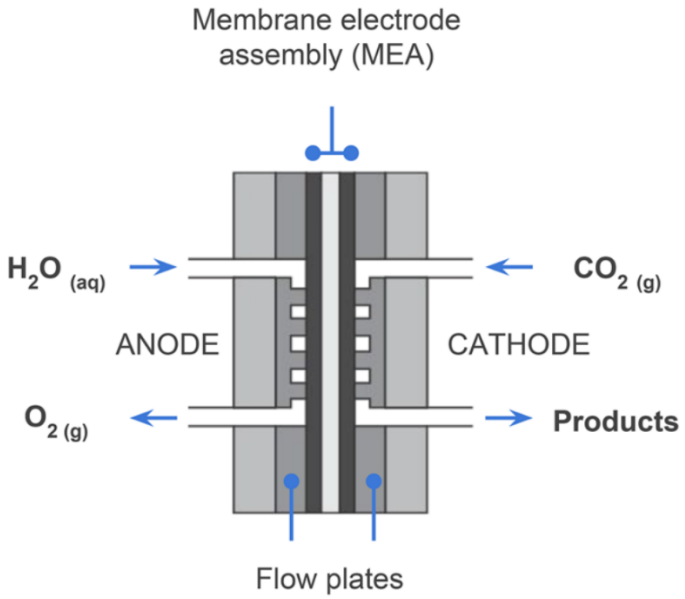

Figure 22: Cross-sectional diagram of an electrolytic CO_2 reduction flow cell[110].

A typical flow cell setup is composed of a cathode where CO_2 is delivered for the reduction, an anode where the electrolysis of water occurs, and a membrane allowing the ionic exchanges.

A concrete example has been presented bellow[112], showing a H_2O and CO_2 electrolysis using new alkaline stable anion membranes, where the reduction of CO_2 to formic acid (HCOOH) occur (**Figure 23**).

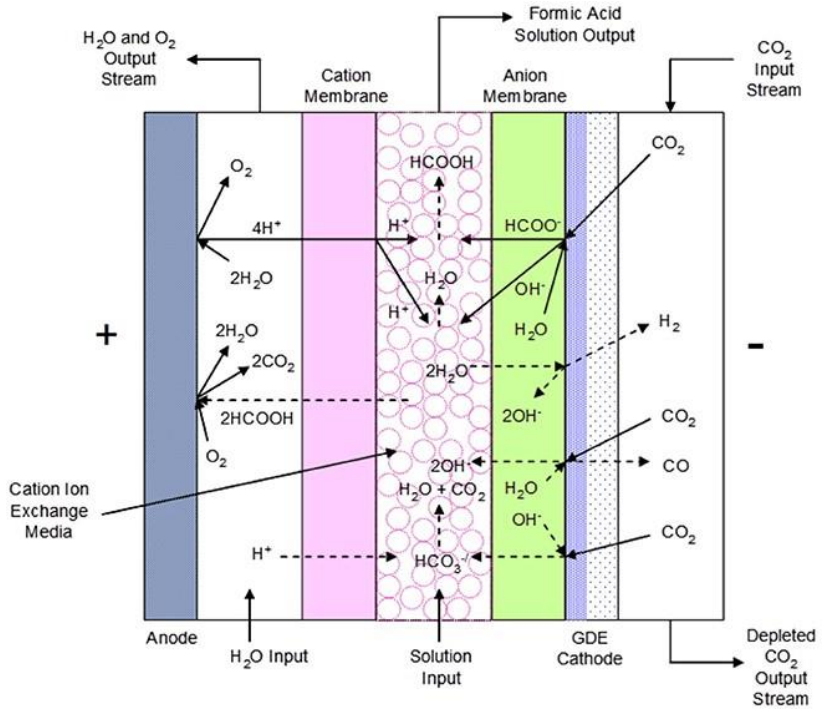

Figure 23: CO_2 - formic acid conversion cell configuration showing reactions and ion transport[112].

The electrochemical reduction of CO_2 occurs at the cathode in the presence of water, generating formate ($HCOO^-$) and hydroxide (OH^-) ions, and at the same time the oxidation of water occurs at the anode, forming oxygen gas and hydrogen ions (hydronium cations H_3O^+) in aqueous solutions. Both formate ions and hydroxide ions migrate through the anion exchange membrane into the centre flow compartment, where they react with hydrogen ions produced in the anode compartment to yield water and formic acid. The hydrogenation of CO_2 to methanol can happen similarly, and the reduction could occur by involving ions or radicals.

The hydrogen molecule may be dissociating following two possible reactions:

$$H^+ + :H^- \rightleftharpoons H_2 \rightleftharpoons H^{\bullet} + {}^{\bullet}H \qquad \textbf{(R2)}$$

In an electrochemical redox reaction, the hydrogen molecule may be dissociating to H^+ and $:H^-$ at the appropriate step, but we chose to explore the radical dissociation only ($H\cdot + \cdot H$), as it is expected to occur just like in most every thermal catalytic hydrogenation.

If radicals are considered instead of hydrogen molecules, the previously discussed aqueous phase mechanism (**Figure 18**) could be redesigned and the effect of a catalyst could be mimicked (**Figure 24**) to give pseudo-catalyzed reaction.

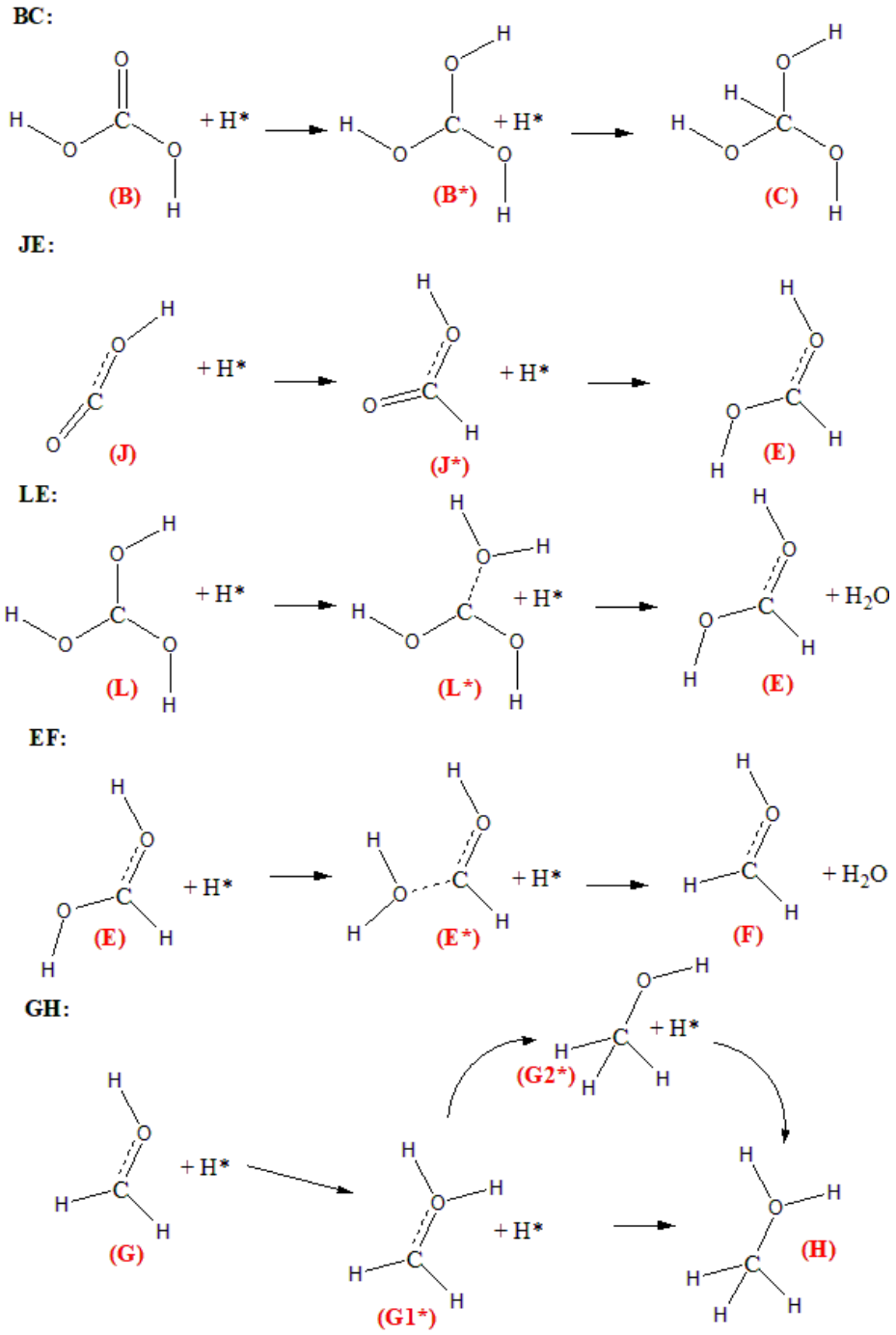

Figure 24: Step-by-step water enhanced CO_2 hydrogenation reaction using hydrogen atoms as a reactant.

The previously described reaction steps (**BC**, **JE**, **LE**, **EF** and **GH**, **Figure 18**) have been replaced by the appropriate hydrogen atom containing steps (**Figure 24**).

A special pseudo-catalyzed mechanism for the hydrogenation of CO_2 to methanol is proposed. The catalytic effect of a metal surface has been mimicked by considering hydrogen atoms instead of hydrogen molecules as reaction partners (**Figure 25**). The presence of water (and

H_3O^+) further enhances the reaction by lowering reaction barriers and thus, behave like additional catalyst even though its effect is modest rather than dramatic.

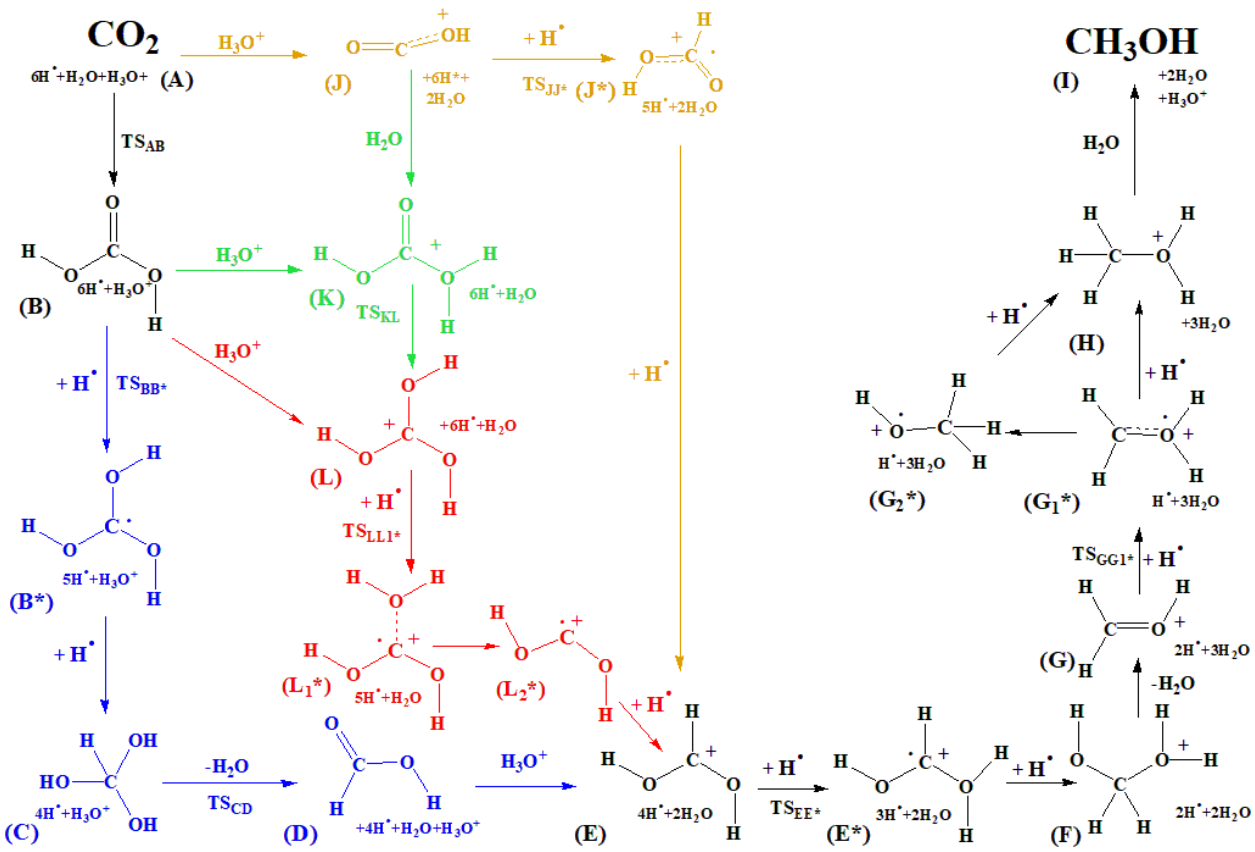

Figure 25: Reaction pathways of the envisaged CO_2 – methanol conversion mechanism using atomic hydrogenations. Letters are assigned to every structure, and each transition state is named as TS followed with the letter referring to the reactant and then the product (*e.g.* **TS$_{AB}$**), respectively. The +H• refers to a hydrogen atom addition.

As a first step CO_2 (**A**) can either be protonated or hydrated and thus, either (**J**) or (**B**) can be formed, respectively. To reach the central compound of the mechanism which is the protonated formic acid **(E)**, four pathways can be followed going through a two-step atomic hydrogenation as follows:

1. **Hydration-hydrogenation route (ABB*CDE**, **Figure 1, *blue*):** by the hydration of CO_2 (**A**) carbonic acid (**B**) will formed (three conformations are possible, the one considered here is energetically higher by 3.14 kJ/mol than the most stable conformer). After that, a sequence of two atomic hydrogenations (**TS$_{BB*}$** and **B*C**) have to occur to produce methanetriol (**C**). Then, a water elimination (**TS$_{CD}$**), leads to formic acid (**D**) and via a protonation step (**E**) is formed.

2. **Protonation-hydrogenation route (AJJ*E, Figure 1, *brown*)**: this route consists of three elementary steps which connects CO_2 with the desired protonated formic acid **(E) intermediate**. A protonation **(AJ)** followed by two atomic hydrogenations **(TS_{JJ*}, J*E)** will lead to **(E)**. It has to be noted that this route is a part of the preferred pathway of the mechanism (the reason will be discussed later).
3. **Hydration-protonation route (ABLL_1*L_2*E, Figure 1, *red*):** this route is diverted from the hydration-hydrogenation route **(*blue*)** after **(B)** is formed. The protonation of carbonic acid (**B**) can **lead to (L)**. Then, the first atomic hydrogenation occurs **(TS_{LL1*}).** After that, a water subtraction **(L_1*L_2*)** followed by the second atomic hydrogenation **(L_2*E)** leads to the protonated formic acid **(E)**.
4. **Protonation-hydrogenation/hydration-protonation route (A[B/J]KLL_1*L_2*E, Figure 1, *green*)**: this route starts with either a protonation **(AJ)** which is followed by a hydration **(JK)** or with a hydration **(TS_{AB})** which is followed by a protonation **(BK)** to reach protonated carbonic acid **(K)**. Then, **(L)** can be formed via a hydrogen shift **(KL)**, which will put this to the track of the ***red*** **(hydration-protonation) route**. From here, **(E)** can be achieved through the reactions **(TS_{LL1*}, L_1*L_2*, L_2*E)** as in the case of the **hydration-protonation route**.

All the routes lead to the formation of **(E)**, protonated formic acid. After that, another two atomic hydrogenations **(TS_{EE*}** and **E*F)** will occur and (**F**) will be formed. Then, a water elimination will lead to (**G**), which is protonated formaldehyde. From here, there are two possible ways to reach **(H)**, and in both cases, the first step would be the formation of **(G1*)**. The shortest way to reach **(H)** is a direct hydrogen atom addition **(G1*H)**. The other way will include the formation of **(G2*)** through a hydrogen shift **(TS_{G1*G2*})**, and then, through a hydrogen atom addition **(G2*H)** the desired intermediate **(H)** will be reached. As a final step, a water mediated proton release **(HI)** will lead to the formation of methanol (**I**) and a hydronium ion. The relative thermodynamic properties of the individual steps have been computed as *e.g.* $\Delta G_r^o = G_{(X)} - G_{ref}$, where $G_{(X)}$ and G_{ref} are the Gibbs free energy of structure X and the reference, respectively (**Figure 26**). The ($CO_2 + 6H^{\bullet} + H_2O + H_3O^+$) are considered as the reference throughout the reaction.

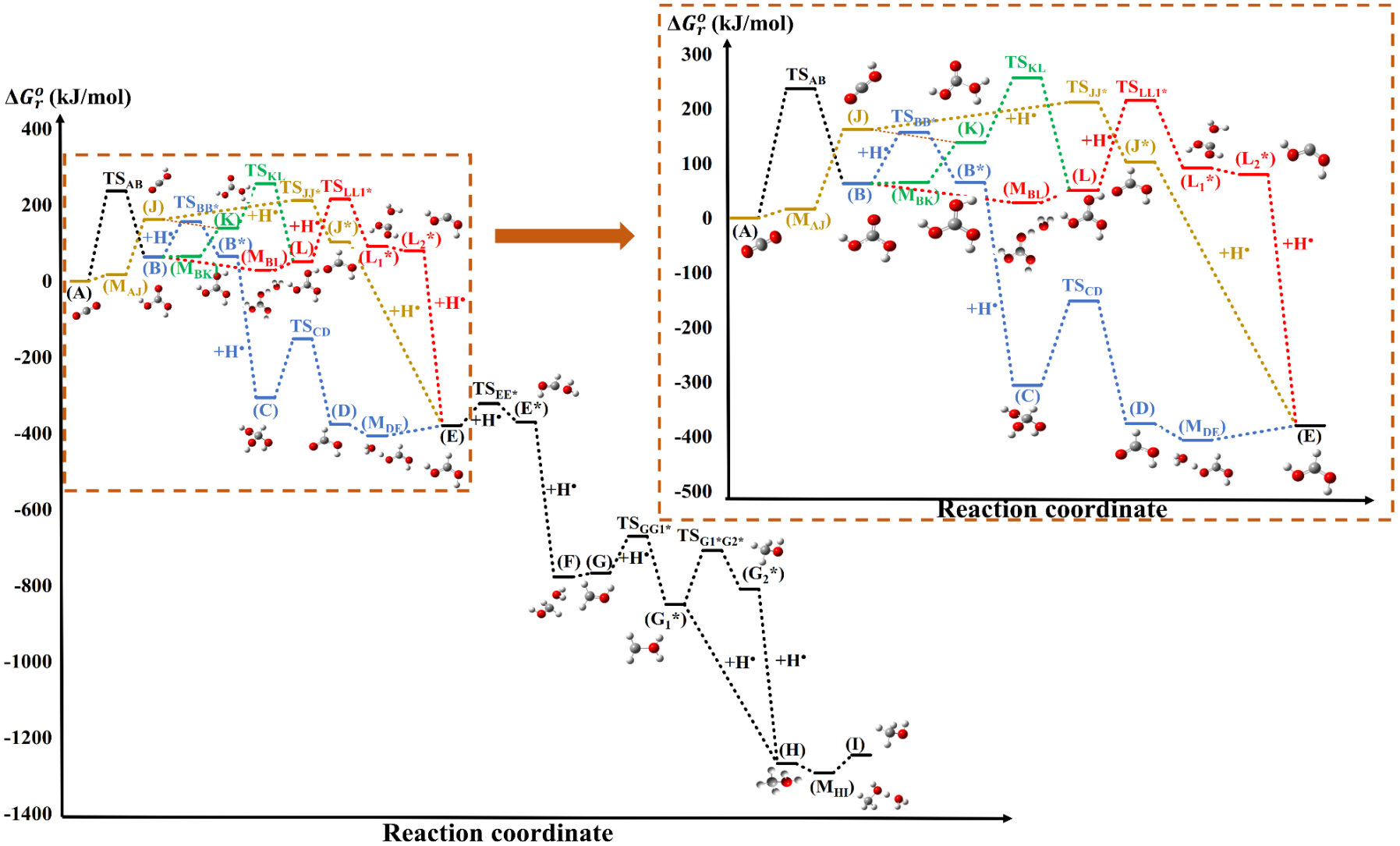

Figure 26: Gibbs free energy change (ΔG_r^o, kJ/mol) of the catalyzed-like aqueous phase mechanism of CO_2 to methanol calculated at W1U combined with the SCRF solvent model. The transition states are named as TS followed by the reactant and the product. The hydrogen additions are highlighted with the (+H) sign close to the barrier. (**B**), (**K**), (**E**) and (**L**) could have more than one conformer.

The mechanism can be divided into two sections: **[A-E]** and **[E-I]** (**Figure 26**). In the section **[A-E]** the conversion of CO_2 (**A**) to protonated formic acid (**E**) could occur through several different pathways. All the routes start (or can start) with a hydration of CO_2 (**A**) to get carbonic acid (**B**) except the **protonation-hydrogenation** (***brown***) pathway. This goes directly from CO_2 (**A**) through a protonation followed by two atomic hydrogenations to the protonated formic acid (**E**) with one single barrier ($\Delta G^{o}_{TS_{JJ^*}}$ = 212.67 kJ/mol). It is the lowest relative energy barrier in the **[A-E]** section, and this makes it the preferred pathway. Thus, the overall preferred pathway would be then: **[A-TS$_{AJ}$-J-TS$_{JJ^*}$-J*-E-TS$_{EE^*}$-E*-F-G-TS$_{GG1^*}$-G1*-H-I]**.

Through the **hydration-hydrogenation** (**Figure 26**, ***blue***) pathway **(E)** could be reached within 5 reaction steps. The highest relative barrier height here is 237.28 kJ/mol which corresponds to (**TS$_{AB}$**). There are two other transition states which are more preferred and their relative Gibbs free energies are significantly lower (**TS$_{BB^*}$**, $\Delta G^{o}_{TS_{BB^*}}$= 156.97 kJ/mol and **TS$_{CD}$**, $\Delta G^{o}_{TS_{CD}}$= -151.49 kJ/mol)**.** This pathway involves also an immediate hydrogen atom addition **(B*C)** and a barrierless reaction with an intermediate **(M$_{DE}$)** having the lowest relative energy value (ΔG^{o}_{DE}= -406.09 kJ/mol) in the **[A-E]** section.

Protonated formic acid (**E**) can also be reached through 5 reaction steps within the **hydration-protonation** (**Figure 26,** ***red***) pathway. The first step is the same as before **(TS$_{AB}$)**, which is followed by a barrierless processes which includes an intermediate **(M$_{BL}$)**. Then, two atomic hydrogenations occur, with a barrierless water removal reaction in between **(L$_1$*L$_2$*)**. The first atomic hydrogenation goes through **(TS$_{LL1^*}$)** ($\Delta G^{o}_{TS_{LL^*}}$= 216.31 kJ/mol), while the second **(L*E)** is a barrierless step. It is possible to link the **protonation-hydrogenation** (***brown***) and **hydration-protonation** (***red***) pathways through a hydration (**JK**) followed by a hydrogen shift (**TS$_{KL}$**, $\Delta G^{o}_{TS_{KL}}$ = 256.78 kJ/mol) which has the highest relative energy among all the routes. This TS is a part of the ***green*** reaction channel as well.

The **[E-I]** is one single route where (**E**) will be converted to methanol (**I**) after 6 consecutive reaction steps or 7 if the side reaction between (**G1***) and (**G2*)** is considered. The relative Gibbs free energy difference between these two molecules ($\Delta\Delta G^{0}_{(G2^*\text{-}G1^*)}$) is 40 kJ/mol, but since **TS$_{GG1^*}$>TS$_{G1^*G2^*}$**, a preferred side reaction route cannot be chosen as both processes could occur. It has to be mentioned that in some cases several conformers can be formed, and several transition states leading to these

conformers are possible. In each case, the most appropriate conformer has been chosen and included into the discussion. Among all the consecutive hydrogen atom additions, the second step is always a barrierless radical recombination reaction (Morse potential). Therefore, the second hydrogen atom in each case, is attached to the rest of the molecule without any additional energy needed (**Figure 27**).

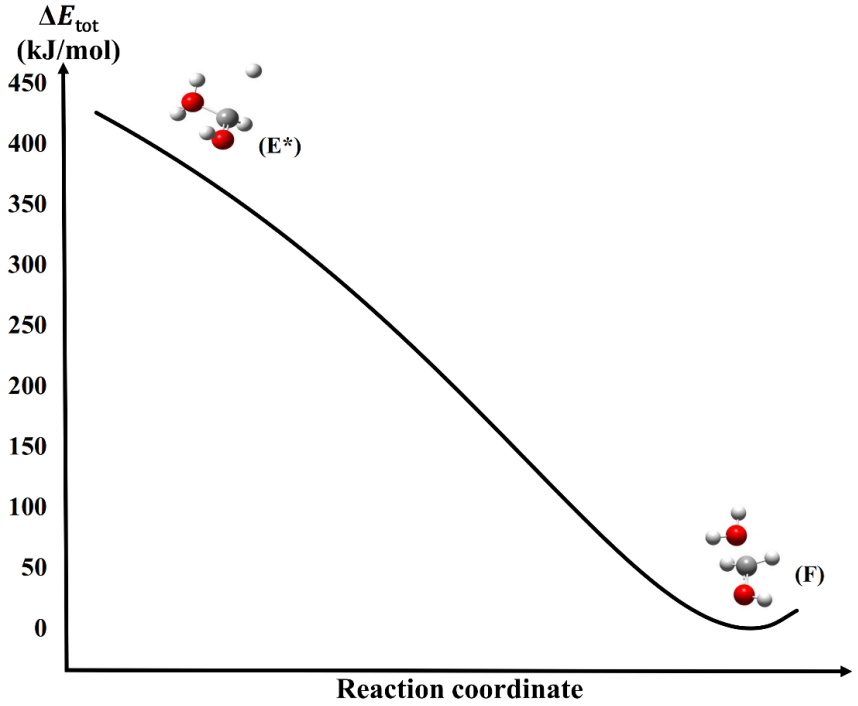

Figure 27: Total energy change (ΔE_{tot}) of the (**E*F**) barrierless reaction step (Morse potential) calculated at the W1U level of theory combined with the SCRF solvent model.

There are six barrierless atomic hydrogenation steps (also known as radical recombination), **(B*C)**, **(L_2*E)**, **(J*E)**, **(E*F)**, **(G_1*H)** and **(G_2*H)**. There were also barrierless water addition/subtraction reactions such as **(JK), (L_1*L_2*)** and **(FG)**. The association of two Morse potentials is another barrierless reaction type involved in the discussed mechanism. Instead of going through a transitions stat, this reaction contains a minimum comprised of a molecular complex such as **(M_{AJ})**, **(M_{BK})**, **(M_{BL})**, **(M_{DE})** or **(M_{HI})**. All of these reactions are protonations and thus the intermediate complexes are always formed by the starting structure and an oxonium ion (H_3O^+). To show the energetic properties of these barrierless reaction steps, **(E*F)** have been examined in detail (**Figure 27**) and the corresponding total energy change has been computed.

The total energy decreases from the reactant's energy level **(E*)** directly to the energy level of the product **(F)** without going through a barrier. The energy level of the product has been considered as a reference for the calculation of the total energy change.

Table 10: Thermodynamic properties (ΔH_r^o, ΔG_r^o in kJ/mol and S in J/mol*K) of the catalyzed-like carbon dioxide – methanol conversion reaction mechanism have been calculated at the W1U level of theory combined with the SCRF solvent model. The complexes formed during barrierless reactions and corresponds to double Morse potentials are noted as M followed by the letter of the reactant and then the product (*e.g.* **M_{AJ}**). The species labelled with an (*) and highlighted in red are involved in the atomic hydrogenations.

Species		ΔH_r^o	ΔG_r^o	S
		kJ/mol		J/mol*K
A	CO_2	0.00	0.00	0.00
B	H_2CO_3	23.96	63.41	-132.32
B*	H_2CO_3-H	**-1.01**	**65.48**	**-223.01**
C	$HC(OH)_3$	-408.42	-306.14	-343.05
D	HCOOH	-434.26	-376.27	-194.51
E	$HCOOH_2^+$	-441.03	-379.69	-205.74
L_1*	$HCOOH^+$-H_2O	**26.50**	**92.01**	**-219.70**
L_2*	$HOCOH^+$	**54.20**	**79.77**	**-85.74**
J	HCO_2^+	166.11	162.31	12.74
J*	$H_2CO_2^+$	**77.18**	**102.99**	**-86.54**
E*	$HCOH^+$-H_2O	**-458.97**	**-370.40**	**-297.07**
F	H_2COH^+-H_2O	-901.29	-777.71	-414.51
G	H_2COH^+	-847.90	-767.68	-269.07
G1*	H_2COH^+-H	**-957.84**	**-849.56**	**-363.18**
G2*	H_3COH^+	**-918.46**	**-809.17**	**-366.58**
H	$H_3COH_2^+$	-1411.50	-1267.97	-481.40
I	H_3COH	-1386.75	-1245.43	-473.98
k	$H_3CO_3^+$	98.83	138.67	-133.64
L	$C(OH)_3^+$	7.97	50.75	-143.48
TS_{AB}	A ⟶ B	197.86	237.28	-132.23
TS_{BB*}	B ⟶ B*	**87.24**	**156.97**	**-233.89**
TS_{CD}	C ⟶ D	-255.65	-151.49	-349.37
TS_{LL*}	L ⟶ L*	**144.20**	**216.31**	**-241.86**
TS_{JJ*}	J ⟶ J*	**188.90**	**212.67**	**-79.70**
TS_{EE*}	E ⟶ E*	**-412.56**	**-321.32**	**-306.03**
TS_{GG1*}	G ⟶ G1*	**-780.73**	**-670.72**	**-369.00**
TS_{G1*G2*}	G1* ⟶ G2*	**-818.20**	**-707.39**	**-371.66**
TS_{KL}	K ⟶ L	213.66	256.78	-144.65
M_{DE}	D-H_3O^+	-503.06	-406.09	-325.24
M_{BL}	B-H_3O^+	-49.12	28.49	-260.30
M_{AJ}	A-H_3O^+	-13.29	17.08	-101.89
M_{HI}	H-H_3O^+	-1472.85	-1292.99	-603.24
M_{BK}	B- H_3O^+	-9.17	65.54	-250.56

After choosing 200 kJ/mol as an arbitrary reference for high energy structures, four transition states have been found which are above this limit, $\Delta G^o_{TS_{AB}}$= 237.28 kJ/mol, $\Delta G^o_{TS_{LL*}}$= 216.31 kJ/mol, $\Delta G^o_{TS_{JJ*}}$= 212.67 kJ/mol and $\Delta G^o_{TS_{KL}}$= 256.78 kJ/mol (**Table 10**). The corresponding reaction steps are a hydration (**TS_{AB}**, water molecule

addition), two atomic hydrogenations (H atom addition, **TS_{LL^*}** and **TS_{JJ^*}**) and a hydrogen atom shift (**TS_{KL}**).

It is possible to calculate the energy storage efficiency (η) of the preferred pathway (**Protonation-hydrogenation,** ***brown***) as follows:

$$\eta = \frac{|\Delta H_r^o|}{\Delta H_{TS}^{max}} = \frac{|\Delta H_{H3COH}^o|}{\Delta H_{TS_{JJ^*}}} \qquad (4)$$

This corresponds to the ratio of the stored enthalpy $|\Delta H_r^o|$ (ΔH_{H3COH}^o = -1386.75 kJ/mol) and the invested enthalpy (the relative enthalpy of the transition state with the highest relative activation energy of the reaction path ΔH_{TS}^{max} is equal to $\Delta H_{TS_{JJ^*}}$= 188.90 kJ/mol). However, in this way, the theoretical efficiency of methanol formation is 734.1 %, which is not possible, as the efficiency would be >100%. However, in this case, the invested energy is not equal to the maximal barrier height only. The energy demand to break three hydrogen-hydrogen bonds (Bond Dissociation Energy of H_2, BDE_{H2}) which will provide the 6 hydrogen atoms has to be also taken into account to get the correct efficiency (η_{corr}) as follows:

$$\eta_{corr} = \frac{|\Delta H_{H3COH}^o|}{\Delta H_{TS_{JJ^*}} + 3 * BDE_{H2}} \qquad (5)$$

Calculated BDE_{H2} (436.56 kJ/mol) has been used in the correction, but it was also compared to the experimentally determined value and the difference is <1 kJ/mol (ΔBDE_{H2}= 0.56 kJ/mol[113]), which also verifies the method selection. All in all, $\boldsymbol{\eta_{corr}}$ was found to be equal to 92.5%.

The efficiency increased a lot compare to the uncatalyzed gas phase ($\boldsymbol{\eta}$ = 14.4%)[91] and water enhanced aqueous phase mechanisms ($\boldsymbol{\eta}$ = 27.1%)[105]. Even though, the number of electrons and atoms were kept the same compare to the previous water enhanced case[105], the difference in efficiency arises from the fact that hydrogen molecules were part of the reactant mixture (CO_2+H_2O+H_3O^++3H_2) previously, while in the current catalyzed-like system, H atoms are considered (CO_2+H_2O+H_3O^++6$H^\bullet$). It has to be mentioned that the presence of water (and H_3O^+) will enhance the reaction by lowering reaction barriers. Thus, it acts like a catalyst even though its effect is modest rather than dramatic. The reactant mixture in the catalyzed-like case is less stable compare to the previous system. However, if the reaction occurs at the surface of a metal catalyst, the

hydrogen atoms would be bonded to the catalyst along with the rest of the molecules. Thus, the whole system would be more stable, and the barriers could decrease even more.

3.4 Comparison between the uncatalyzed and the catalyzed-like water enhanced mechanism

The two preferred pathways of the CO_2 conversion to methanol in the uncatalyzed and catalyzed-like mechanisms have been compared (**Table 11**).

Table 11: Comparison of the preferred carbon dioxide-methanol conversion pathways of the water enhanced and catalyzed-like aqueous phase mechanisms.

	Aqueous phase (uncatalyzed)	**Aqueous phase (catalyzed-like)**
Reactant mixture	$CO_2 + 3H_2 + H_2O + H_3O^+$	$CO_2 + 6H^{\bullet} + H_2O + H_3O^+$
Barrierless reactions	Yes	Yes
Ionic reactions	Yes	Yes
Hydrogen atom addition reactions	No	Yes
Highest energy barrier (kJ/mol)	355.52	212.67
Efficiency (η)	27.1%	92.5 %

It has to be emphasized that the mechanisms do not have the same initial reactant mixtures as it was mentioned above. Both mechanisms involve barrierless and ionic reaction steps, but hydrogen atom additions obviously occur only in the catalyzed-like case. In the catalyzed-like pathway, there is only one transition state with a relative barrier higher than 200 kJ/mol ($\Delta G^{o}_{TS_{JJ*}}$= 212.67 kJ/mol). Unlike in the other case, where all the barriers are above > 200 kJ/mol. In the case of the uncatalyzed mechanism the efficiency is 27.1%, which is far lower than what can be achieved with the catalyzed-like mechanism (92.5 %).

A significant decrease of the energy barriers was observed in the overall process compared to the uncatalyzed water enhanced mechanism. A large increase has also been achieved in the energy storage efficiency. The catalyzed-like mechanism is 3.4 times more efficient (92.5%) than the corresponding uncatalyzed process (27.1%). The results are an important step further to understand carbon dioxide hydrogenation and to design new catalysts with better performance.

4 Summary

“All institutes must renew themselves, from time to time, as the price of survival”

Anonymous

We must emphasize that all institutes really mean ALL INSTITUTES since every institutes that were operationally acceptable in the previous phase of global civilization will become obsolete and therefore useless in the next phase of the global civilization. By ALL INSTITUTES we mean education, energy production, material production, food production, medicine, scientific research and development to mention only a few. Finally, this universal law implies that an institute that renewed itself payed the price of survival and can therefore continue to be active in the nearby future; consequently, an institute that doesn’t renew itself doesn’t pay the price of survival, condemns itself to die.

The high-capacity storage of renewable electrical energy can be completed with the Substitute Natural Gas (SNG) alternative. The SNG alternative is the chemical bonding of hydrogen obtained from electrolysis using renewable electricity to carbon dioxide, which can be obtained from several sources. This will almost certainly contribute to the reduction of the emission of these species into the atmosphere. However, the conversion of CO_2 to methanol is a rather complicated multistep process. The chemical reduction of carbon dioxide has several reaction steps and a multitude of intermediate products. Newly developed uncatalyzed and catalyzed-like mechanisms have been proposed and thermodynamically investigated in both the gas and aqueous phases using computational chemistry tools. The Gibbs free energy change of the most favorable pathways of both mechanisms are shown in **Figure 28**.

By comparing the uncatalyzed gas phase and aqueous phase processes the following conclusions can be drawn:

- In both cases, hydrogenation reactions have the highest energy barriers.
- The highest energy barriers in the preferred pathways of the two mechanisms are equal to $\boldsymbol{\Delta G_{(Gas)}}$ **= 400.66 kJ/mol** and $\boldsymbol{\Delta G_{(Aqueous)}}$ **= 355.52 kJ/mol**.
- The aqueous phase mechanism is almost two times more efficient than the gas phase ($\boldsymbol{\eta_{(Aqueous)} = 27.1\%}$ *vs* $\boldsymbol{\eta_{(Gas)} = 14.4\%}$).

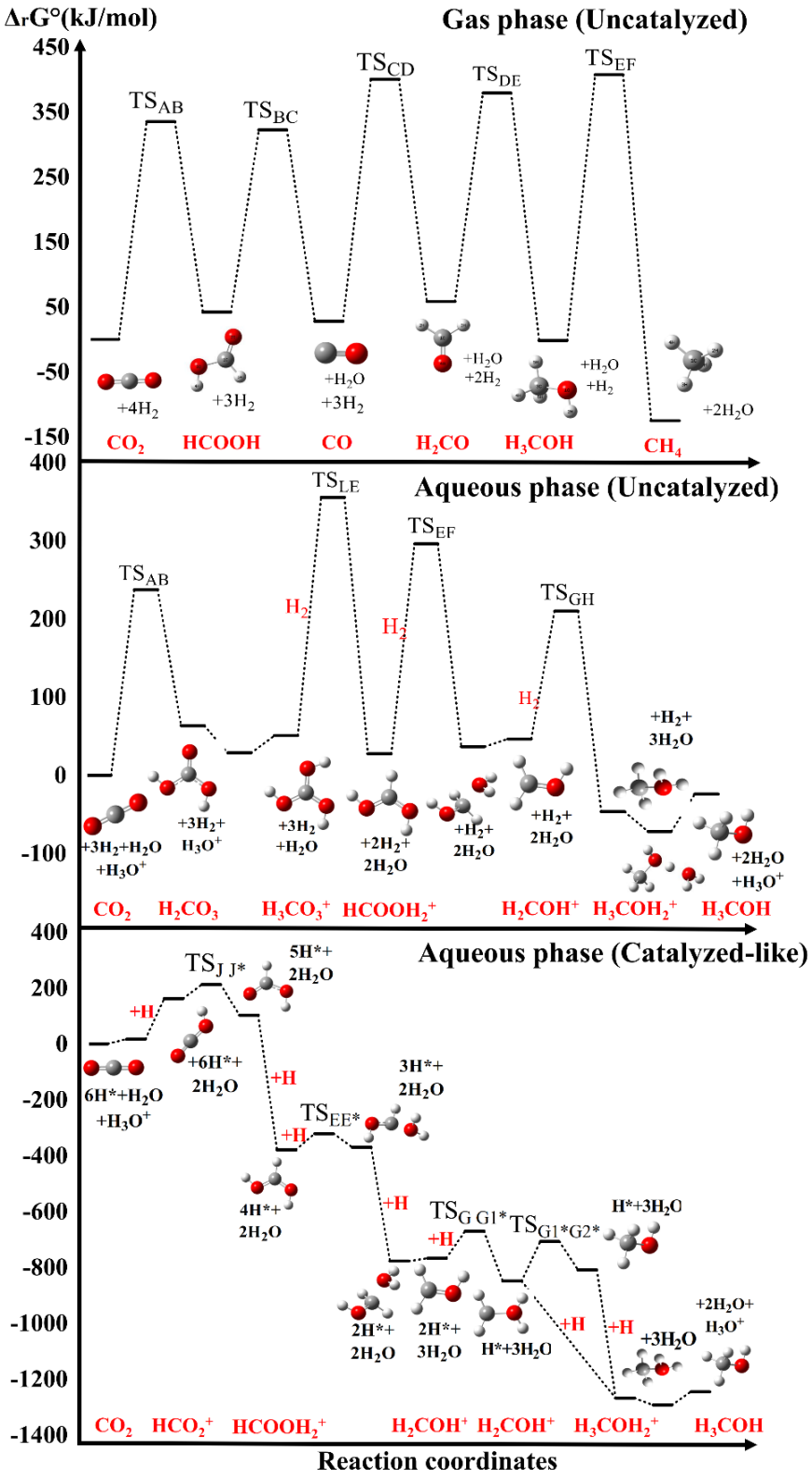

Figure 28: Gibbs free energy change of the preferred pathways of the gas phase and aqueous phase uncatalyzed mechanism, and catalyzed-like process.

We notice that in the gas phase mechanism (**Figure 28,** top) the reaction barriers are the highest between the three PESs. In the preferred pathway of the aqueous phase mechanism (**Figure 28,** middle) the energy barriers are already lower.

The efficiencies of each process can be increased by lowering the energy barriers of the hydrogenation steps. This can be achieved using hydrogen atoms as reactants instead of hydrogen molecules, which can be facilitated by employing a catalyst or an electrocatalytic systems.

Since the water enhanced aqueous phase mechanism has the highest efficiency, it was used as a starting point. Hydrogen molecules have been replaced by hydrogen atoms and a catalyzed-like mechanism have been designed and the preferred pathway has been selected (**Figure 28**, bottom).

After analyzing the catalyzed-like mechanism, further improvement and a significant decrease of the energy barriers was observed in the overall process and the corresponding energy barriers are significantly lowered. In the preferred pathway, the highest barrier is only equal to $\boldsymbol{\Delta G_{(\mathbf{H}*)}}$= 212.67 kJ/mol which compared to the uncatalyzed mechanism, is almost twice smaller. Thus, a considerable increase has been achieved in the efficiency. The catalyzed-like mechanism is 3.4 times more efficient than the gas phase non-catalyzed process ($\boldsymbol{\eta_{(\mathbf{H}*)}} = 92.5\%$).

Based on these results, we would recommend a catalyst that has proven efficiency in breaking the H-H bond as the first step in the catalytic conversion of CO2 to methanol, in order to use atomic hydrogen (H•) as a reactant instead of molecular hydrogen (H2). Moreover, the inclusion of a super acid in the reaction mechanism may also enhance this process by facilitating ionic barrierless reactions. If the scientific community succeeds in finding a cheap and innovative environmentally-friendly technology able to efficiently convert CO_2 to added-value products such as methanol, they could provide solutions to environmental problems such as the emission of carbon dioxide in the atmosphere. This would enable the production, storage, and transport of energy to finally be sustainable. Concerned scientists can then focus exclusively on studying potential methods for capturing and converting the carbon dioxide already present in nature.

5 New scientific results

“Books are like mirrors: if a fool looks in, you cannot expect a genius to look out.”

J.K. Rowling

1st Thesis

Several uncatalyzed reaction routes of CO_2 to methanol conversion have been designed and studied in gas phase where **9** intermediate molecular complexes were involved (**Figure 16**). The thermochemical properties have been computed and the potential energy surfaces (PES) have been proposed (**Figure 17**). Among the multitude of potential pathways, the most favourable ones have been selected and discussed. We have shown that the uncatalyzed gas phase CO_2 hydrogenation is thermodynamically unavailable considering the size of its rate determining step $\boldsymbol{\Delta G_{(Gas)}}$= 400.66 kJ/mol.

2nd Thesis

In the newly proposed uncatalyzed aqueous phase CO_2 reduction mechanism (**Figure 18**), the energy barriers are significantly lower than in the gas phase (about 100 kJ/mol lower). The most favorable route has been identified within the aqueous phase catalyzed-like hydrogenation mechanism. Therein lies only one barrier above 300 kJ/mol ($\boldsymbol{\Delta G_{(Aqueous)}}$= 355.52 kJ/mol).

3rd Thesis

Further improvement marked by a significant reduction of the energy barriers was observed in the catalyzed-like mechanism (**Figure 25**), where the highest energy barrier is only equal to $\boldsymbol{\Delta G_{(H\bullet)}}$= 212.67 kJ/mol. Based on the energetics and the calculated efficiencies, it can be concluded that the atomic hydrogenation mechanism is a key process for CO_2 reduction, because of its relatively low energy barriers and high efficiency ($\boldsymbol{\eta_{(H\bullet)} = 92.5\ \%}$). This mechanism can be achieved by using appropriately selected/designed catalysts or electrocatalytic systems.

4th Thesis

We have introduced the concept of energy storage efficiency. This allows us to compare the most favourable pathways of the conversion of CO_2 to methanol under different conditions. The aqueous phase mechanism is more efficient than the gas phase mechanism. Its efficiency is almost the double than the gas phase case: $\boldsymbol{\eta_{(Aqueous)} = 27.1\%}$ *vs* $\boldsymbol{\eta_{(Gas)} = 14.4\%}$. Mimicking the catalytic process in the aqueous phase leads to an enormous increase and it is 3.4 times more efficient than the water enhanced non-catalyzed process ($\boldsymbol{\eta_{(H*)} = 92.5\ \%.}$).

5th Thesis

The W1 composite method has been selected for all calculations and its applicability to describe the thermochemistry of the studied processes (and other similar reactions) has been verified. The method has been tested and compared to experimental values. The average deviation observed from the experimental results is **1.61** kJ/mol (**0.39** kcal/mol).

6 Scientific publications

“Life is a train that stops at no stations; you either jump abroad or stand on the platform and watch as it passes”

Yasmina Khadra

Journal of Cleaner Production 241 (2019) 118221

Contents lists available at ScienceDirect

Journal of Cleaner Production

journal homepage: www.elsevier.com/locate/jclepro

Renewable energy and raw materials – The thermodynamic support

Rachid Hadjadj, Csaba Deák, Árpád Bence Palotás, Péter Mizsey*, Béla Viskolcz

University of Miskolc, Miskolc-Egyetemváros, H-3515, Miskolc, Hungary

ARTICLE INFO

Article history:
Received 22 January 2019
Received in revised form
22 August 2019
Accepted 28 August 2019
Available online 4 September 2019

Handling editor: Prof. Jiri Jaromir Klemeš

Keywords:
Carbon dioxide hydrogenation
Methane
Methanol
Thermodynamic study
Energy storage

ABSTRACT

The energy and raw material supplies are crucial issues in our societies. The possible solution of these issues can be coupled with the storage alternatives of renewable energy. The chemical way of energy storage can be quite different but we follow the Supplement of Natural Gas concept since this delivers a high storage capacity solution. The chemical way of energy storage is based on the carbon dioxide hydrogenation. It is in agreement with the theory of the circular economy so that the carbon emission is reduced with the concept of Carbon Capture and Utilization (CCU).

In this work the reaction system of the carbon dioxide hydrogenation is studied thermodynamically applying the tool of quantum chemistry. The aim of the study is to support the carbon dioxide transformation alternatives of industrial scale, that is, the CCU. It is determined that the methane production has the highest thermodynamic efficiency where the methanol production is the second in the ranking. These thermodynamic efficiencies are 14.4% for methanol and 44.4% for methane. Both alternatives have, however, advantages since the methane can be introduced directly into the natural gas network and the methanol has the highest volumetric energy content. Both molecules can be transformed into different kind of raw materials, see e.g. methanol economy. At the selection, however, other, practical points of view should be also considered where industrial experiences and circumstances are to be also taken into account.

Having recognized the need to deal with the reduction and utilization of carbon dioxide emission (CCU), the University of Miskolc established the "Environmental Carbon Dioxide Partnership". It has several industrial partners having significant carbon dioxide emission and therefore experience in this issue. The experts of the partnership help to solve emission problems and the carbon dioxide utilization, based on the theoretical and practical results and experiences of the Partnership. This thermodynamic investigation supports the development of the Partnership to carry out the most efficient CCU method.

1. Introduction

The harmful effect of the carbon dioxide emitted into the atmosphere is a well-known issue (Vo et al., 2019). To answer the challenges of environmental protection, University of Miskolc, Hungary, established a network called "Environmental Carbon dioxide Partnership" aiming to contribute to

- the global warming problem (Chandler, 2018),
- storage of renewable energies (Banerjee et al., 2019),
- production of materials on renewable basis (Islam et al., 2018).

To complete these goals the carbon dioxide can be the key molecule, the so-called platform molecule that is used for the solution of these challenges. The carbon dioxide can be chemically converted into different molecules for the sake of energy storage like formic acid, formic aldehyde, methanol or methane (Leonzio, 2018). These molecules can be used not only for the storage and production of energy but to produce other chemicals on renewable basis (Markewitz et al., 2012).

The three goals of the Partnership are associated with the energy and energy production. Energy, the basic element that every nation need, is now a debated subject pushing the scientific world to look for its sustainable forms considering its declining resources combined with the increasing demand as well as the environmental impact (Matthews et al., 2018).

It is important to note that the large capacity energy storage is badly needed for the extensive use of renewable electricity. The reason is that the renewable electricity production highly depends

* Corresponding author.
E-mail address: kemizsey@uni-miskolc.hu (P. Mizsey).

https://doi.org/10.1016/j.jclepro.2019.118221
0959-6526/

Chemical Physics Letters 746 (2020) 137298

Contents lists available at ScienceDirect

Chemical Physics Letters

journal homepage: www.elsevier.com/locate/cplett

Research paper

Water enhanced mechanism for CO_2 – Methanol conversion

Rachid Hadjadj[a], Imre G. Csizmadia[a,c], Péter Mizsey[a], Svend Knak Jensen[d], Béla Viskolcz[a], Béla Fiser[a,b,*]

[a] Institute of Chemistry, University of Miskolc, 3515 Miskolc-Egyetemváros, Hungary
[b] Ferenc Rákóczi II. Transcarpathian Hungarian Institute, 90200 Beregszász, Transcarpathia, Ukraine
[c] Department of Chemistry, University of Toronto, Toronto, M5S 1A1 Ontario, Canada
[d] Department of Chemistry, Langelandsgade 140, Aarhus University, DK-8000 Aarhus C, Denmark

HIGHLIGHTS

- CO_2–CH_3OH conversion in aqueous phase has been envisaged: (CO_2 + $3H_2$ + H_2O + H_3O^+).
- The reaction has been investigated by using the high level W1U composite method.
- Hydrogenations are the least favourable steps in the reaction.
- The energy storage efficiency of the studied mechanism is 27.1%.
- Catalysts can be designed to decrease the energy barrier and increase efficiency.

ARTICLE INFO

Keywords:
Carbon dioxide hydrogenation
Climate change
Computational study
Energy storage

ABSTRACT

Carbon dioxide can be converted into fine chemicals such as methanol and thus, the produced renewable energy can be stored in chemical bonds through reductions. To achieve this, a water enhanced mechanism of CO_2 hydrogenation leading to methanol has been designed by applying 1:3 (CO_2 + $3H_2$) extended with a water molecule and a hydronium. The thermodynamic properties of the intermediate species and transition states have been calculated by using the W1U composite method. The energy efficiency of the studied mechanism is 27.1%. By understanding the mechanism, special purpose catalysts can be designed to accelerate carbon dioxide conversion.

1. Introduction

It is widely known that carbon dioxide (CO_2) release in nature has a detrimental effect, and research in environmental protection is a challenge nowadays [1]. Since the industrial revolution, CO_2 emissions did not stop increasing [2], which could be one of the possible factors behind global warming and the acidification of the oceans [3]. These adverse processes should be prevented by either inhibiting the release or developing large scale carbon dioxide capturing procedures. Most of the solutions proposed till now are mainly Carbon Capture and Storage (CCS) methods, which are not definitive solutions to eradicate the excess of CO_2 from the atmosphere [4]. Some ocean scientists think that ocean storage of CO_2 might be a good idea. In this case, the gas would be injected and trapped into the deep ocean [5], but will it stay there forever? Will it not be able to diffuse? From a chemical point of view, the best solution would be the total transformation of carbon dioxide into added value products [6], and in this way the produced renewable energy can also be stored [7]. Renewable energy production is not stable, and highly depends on the weather and other factors, and the energy consumption fluctuates as well, which means that the energy storage is unavoidable [8]. The common solution to both of these problems is to use renewable energy to convert carbon dioxide chemically into different molecules such as formic acid, formaldehyde, methanol or methane for the sake of energy storage [9]. These molecules can be used not only for the storage and production of energy, but to produce other chemicals in a renewable basis [10]. Energy will be stored in chemical bonds by recycling of carbon dioxide via hydrogenative reductions, and the hydrogen would be obtained from electrolysis using renewable electrical energy [11], which ideally will contribute to the decrease of CO_2 emission [12]. Carbon dioxide can be collected from several sources such as the industrial or biochemical processes [13], and the hydrogen has also many possible sources such

* Corresponding author.
E-mail address: kemfiser@uni-miskolc.hu (B. Fiser).

https://doi.org/10.1016/j.cplett.2020.137298
Received 11 January 2020; Received in revised form 18 February 2020; Accepted 1 March 2020
Available online 02 March 2020

Journal publications

1. Rachid Hadjadj, Csaba Deák, Árpád Bence Palotás, Péter Mizsey, Béla Viskolcz, Renewable energy and raw materials – The thermodynamic support, *Journal of Cleaner Production*, doi:10.1016/j.jclepro.2019.118221. (**Q1; IF = 6.395**)
2. Rachid Hadjadj, Imre G.Csizmadia, Péter Mizsey, Svend Knak Jensen, Béla Viskolcz, Béla Fiser, Water enhanced mechanism for CO_2 – Methanol conversion, *Chemical Physics Letters*, doi:10.1016/j.cplett.2020.137298. (**Q2; IF = 2.291**)
3. Rachid Hadjadj, Imre G.Csizmadia, Péter Mizsey, Béla Viskolcz and Béla Fiser, Catalysed-like mechanism for CO_2 conversion to methanol, Arabian Journal of Chemistry, under review, **2020**.

Oral and Poster presentations

1. 9th Visegrad Symposium on Structural Systems Biology, Water catalysed reduction of CO_2 to methanol in Aqueous-phase, Szilvásvárad, Hungary, **2019**, *Poster*.
2. 1st Science Unlimited Conference – Eötvös Symposium, Uncatalyzed molecular network for CO_2 hydrogenation to methanol end methane, Miskolc, Hungary **2019**, *Oral presentation*.
3. 25th International Symposium on Gas Kinetics and Related Phenomena, Detailed molecular network of CO_2 hydrogenation **2018**, Lille, France, *Poster*.
4. Conversion of CO_2 to CH_3OH - A mechanistic study, XXIII. Bolyai Conference, **2018**, Budapest, Hungary, *Poster*.
5. 7th Visegrad Symposium on Structural Systems Biology, Systematic theoretical investigation for high energy $C_2H_8O_4$ molecules, Nove Hrady, Czech Republic, **2017**, *Poster*.

7 References

"When the snows fall and the white winds blow, the lone wolf dies but the pack survives."

George R.R. Martin

[1] M. Stork, J. de Beer, N. Lintmeijer, and B. den Ouden, 1 (2018).

[2] BP, Full Report – BP Statistical Review of World Energy (2019).

[3] H.D. Matthews, K. Zickfeld, R. Knutti, and M.R. Allen, Environ. Res. Lett. **13**, 010201 (2018).

[4] P. Ibarra-Gonzalez and B.G. Rong, Chinese J. Chem. Eng. **27**, 1523 (2019).

[5] I. Dincer and C. Acar, Int. J. Hydrogen Energy **40**, 11094 (2014).

[6] K.K. Rajan, in 2018 Int. Conf. Control. Power, Commun. Comput. Technol. ICCPCCT 2018 (Institute of Electrical and Electronics Engineers Inc., 2018), pp. 107–113.

[7] S. Weitemeyer, D. Kleinhans, T. Vogt, and C. Agert, Renew. Energy **75**, 14 (2015).

[8] G.A. Olah, G.K.S. Prakash, and A. Goeppert, J. Am. Chem. Soc. **133**, 12881 (2011).

[9] G.A. Olah, A. Goeppert, and G.K.S. Prakash, Beyond Oil and Gas: The Methanol Economy (WILEY-VCH, 2006).

[10] A.J. Pain, J.B. Martin, and C.R. Young, Limnol. Oceanogr. (2019).

[11] F.M. Baena-Moreno, M. Rodríguez-Galán, F. Vega, B. Alonso-Fariñas, L.F. Vilches Arenas, and B. Navarrete, Energy Sources, Part A Recover. Util. Environ. Eff. **41**, 1403 (2019).

[12] D.H. Vo, H.M. Nguyen, A.T. Vo, and M. McAleer, Econom. Inst. Res. Pap. (2019).

[13] W. Chandler, Energy and Environment in the Transition Economies (Routledge, 2018).

[14] J.-P. Gattuso and L. Hansson, Ocean Acidification (Oxford University Press, 2011).

[15] A. Raza, R. Gholami, R. Rezaee, V. Rasouli, and M. Rabiei, Petroleum **5**, 335 (2019).

[16] P. Larkin, W. Leiss, and D. Krewski, Int. J. Risk Assess. Manag. **22**, 254 (2019).

[17] E.E. Adams and K. Caldeira, Elements **4**, 319 (2008).

[18] M.T. Islam, N. Huda, A.B. Abdullah, and R. Saidur, Renew. Sustain. Energy Rev. **91**, 987 (2018).

[19] G. Centi, E.A. Quadrelli, and S. Perathoner, Energy Environ. Sci. **6**, 1711 (2013).

[20] J. Banerjee, K. Dutta, and D. Rana, in (Springer, Cham, 2019), pp. 51–104.

[21] G. Leonzio, J. CO2 Util. **27**, 326 (2018).

[22] X.-M. Hu and K. Daasbjerg, Nature **575**, 598 (2019).

[23] C. Steinlechner and H. Junge, Angew. Chemie Int. Ed. **57**, 44 (2018).

[24] A. Xia, X. Zhu, and Q. Liao, in Fuel Cells Hydrog. Prod. (Springer New York, New York, NY, 2019), pp. 833–863.

[25] F. Samimi, N. Hamedi, and M.R. Rahimpour, J. Environ. Chem. Eng. **7**, 102813 (2019).

[26] D. Sheldon, Johnson Matthey Technol. Rev. **61**, 172 (2017).

[27] M. Huš, V.D.B.C. Dasireddy, N. Strah Štefančič, and B. Likozar, Appl. Catal. B Environ. **207**, 267 (2017).

[28] F. (Ferenc) Ruff and I.G. Csizmadia, Organic Reactions : Equilibria, Kinetics, and Mechanism (Elsevier, Amsterdam ;New York, 1994).

[29] M. Huš, V.D.B.C. Dasireddy, N. Strah Štefančič, and B. Likozar, Appl. Catal. B Environ. **207**, 267 (2017).

[30] C. Tisseraud, C. Comminges, T. Belin, H. Ahouari, A. Soualah, Y. Pouilloux, and A. Le Valant, J. Catal. **330**, 533 (2015).

[31] R. Grabowski, J. Słoczyński, M. Śliwa, D. Mucha, R.P. Socha, M. Lachowska, and J. Skrzypek, ACS Catal. **1**, 266 (2011).

[32] S.A. Kondrat, P.J. Smith, L. Lu, J.K. Bartley, S.H. Taylor, M.S. Spencer, G.J. Kelly, C.W. Park, C.J. Kiely, and G.J. Hutchings, Catal. Today (2018).

[33] P. Gao, L. Zhong, X. Li, H. Wang, H. Yang, C. Zhang, S. Wang, W. Wei, and Y. Sun, (2017).

[34] S. YANG, J. HE, N. ZHANG, X. SUI, L. ZHANG, and Z. YANG, J. Fuel Chem. Technol. **46**, 179 (2018).

[35] P. Gao, L. Zhong, L. Zhang, H. Wang, N. Zhao, W. Wei, and Y. Sun, Catal. Sci. Technol. **5**, 4365 (2015).

[36] J. Toyir, R. Miloua, N.E. Elkadri, M. Nawdali, H. Toufik, F. Miloua, and M. Saito, Phys. Procedia **00**, 0 (2008).

[37] N. Austin, J. Ye, and G. Mpourmpakis, Catal. Sci. Technol. **7**, 2245 (2017).

[38] S. Kattel, B. Yan, Y. Yang, J.G. Chen, and P. Liu, J. Am. Chem. Soc. **138**, 12440 (2016).

[39] P. Xu, K. Ye, M. Du, J. Liu, K. Cheng, J. Yin, G. Wang, and D. Cao, RSC Adv. **5**, 36656 (2015).

[40] B. An, J. Zhang, K. Cheng, P. Ji, C. Wang, and W. Lin, J. Am. Chem. Soc. **139**, 3834 (2017).

[41] Y. Hartadi, D. Widmann, and R.J. Behm, Phys. Chem. Chem. Phys. **18**, 10781 (2016).

[42] H. Bahruji, M. Bowker, G. Hutchings, N. Dimitratos, P. Wells, E. Gibson, W. Jones, C. Brookes, D. Morgan, and G. Lalev, J. Catal. **343**, 133 (2016).

[43] H. Bahruji, R.D. Armstrong, J. Ruiz Esquius, W. Jones, M. Bowker, and G.J. Hutchings, Ind. Eng. Chem. Res. acs. iecr.8b00230 (2018).

[44] J. Díez-Ramírez, P. Sánchez, A. Rodríguez-Gómez, J.L. Valverde, and F. Dorado, Ind. Eng. Chem. Res. **55**, 3556 (2016).

[45] J. Díez-Ramírez, J.A. Díaz, P. Sánchez, and F. Dorado, J. CO2 Util. **22**, 71 (2017).

[46] J. Qu, X. Zhou, F. Xu, X.-Q. Gong, and S.C.E. Tsang, J. Phys. Chem. C **118**, 24452 (2014).

[47] A. García-Trenco, E.R. White, A. Regoutz, D.J. Payne, M.S.P. Shaffer, and C.K. Williams, ACS Catal. **7**, 1186 (2017).

[48] I. Sharafutdinov, C.F. Elkjær, H.W. Pereira de Carvalho, D. Gardini, G.L. Chiarello, C.D. Damsgaard, J.B. Wagner, J.-D. Grunwaldt, S. Dahl, and I. Chorkendorff, J. Catal. **320**, 77 (2014).

[49] Y. Chen, S. Choi, and L.T. Thompson, J. Catal. **343**, 147 (2016).

[50] A. García-Trenco, A. Regoutz, E.R. White, D.J. Payne, M.S.P. Shaffer, and C.K. Williams, Appl. Catal. B Environ. **220**, 9 (2018).

[51] D. Sheldon, Johnson Matthey Technol. Rev. **61**, 172 (2017).

[52] M. Born and J.R. Oppenheimer, Ann. Phys. 84, 457 (1927).

[53] A. Leach, Molecular Modelling : Principles and Applications, 2nd ed. (Prentice Hall, Harlow England ;;New York, 2001).

[54] D. Hartree, Math. Proc. Cambridge Philos. Soc. **24**, 89 (1928).

[55] Roothaan C.C.J., **23**, 69 (1951).

[56] C. Møller and M.S. Plesset, **46**, 618 (1934).

[57] M.J. Frisch, M. Head-Gordon, and J.A. Pople, Chem. Phys. Lett. **166**, 275 (1990).

[58] J.A. Pople, M. Head-Gordon, and K. Raghavachari, J. Chem. Phys. **87**, 5968 (1987).

[59] R.J. Bartlett and G.D. Purvis, Int. J. Quantum Chem. **14**, 561 (1978).

[60] G.D. Purvis and R.J. Bartlett, J. Chem. Phys. **76**, 1910 (1982).

[61] W. Kohn, A.D. Becke, and R.G. Parr, J. Phys. Chem. **100**, 12974 (1996).

[62] B.G. Johnson, P.M.W. Gill, and J.A. Pople, J. Chem. Phys. **98**, 5612 (1993).

[63] A.D. Becke, J. Chem. Phys. **98**, 5648 (1993).

[64] P. Review, Phys. Rev. A **38**, 3098 (1988).

[65] C. Lee, C. Hill, and N. Carolina, **37**, (1988).

[66] D. Samuel, J. Hepatol. **56**, 4 (2012).

[67] A.D. Becke, J. Chem. Phys. **140**, (2014).

[68] E.R. Davidson and D. Feller, Chem. Rev. **86**, 681 (1986).

[69] R. Ditchfield, W.J. Hehre, and J.A. Pople, J. Chem. Phys. **54**, 724 (1971).

[70] R. Ditchfield, W.J. Hehre, and J.A. Pople, J. Chem. Phys. **54**, 724 (1971).

[71] V.A. Rassolov, M.A. Ratner, J.A. Pople, P.C. Redfern, and L.A. Curtiss, J. Comput. Chem.

22, 976 (2001).

[72] T.H. Dunning, J. Chem. Phys. **90**, 1007 (1989).

[73] J.A. Pople, M. Head-Gordon, D.J. Fox, K. Raghavachari, and L.A. Curtiss, J. Chem. Phys. **90**, 5622 (1989).

[74] J.W. Ochterski, G.A. Petersson, and J.A. Montgomery, J. Chem. Phys. **104**, 2598 (1996).

[75] E.C. Barnes, G.A. Petersson, J.A. Montgomery, M.J. Frisch, and J.M.L. Martin, J. Chem. Theory Comput. **5**, 2687 (2009).

[76] P. Pulay, G. Fogarasi, F. Pang, and J.E. Boggs, J. Am. Chem. Soc. **101**, 2550 (1979).

[77] M.P. Andersson and P. Uvdal, J. Phys. Chem. A **109**, 2937 (2005).

[78] R.E. Skyner, J.L. McDonagh, C.R. Groom, T. Van Mourik, and J.B.O. Mitchell, Phys. Chem. Chem. Phys. **17**, 6174 (2015).

[79] B. Mennucci and R. Cammi, Continuum Solvation Models in Chemical Physics: From Theory to Applications (Wiley Online Library, n.d.).

[80] M. J. Frisch, G. W. Trucks, H. B. Schlegel, G. E. Scuseria, M. A. Robb, J. R. Cheeseman, G. Scalmani, V. Barone, G. A. Petersson, H. Nakatsuji, X. Li, M. Caricato, A. Marenich, J. Bloino, B. G. Janesko, R. Gomperts, B. Mennucci, H. P. Hratchian, J. V. Ortiz, A. F. Izmaylov, J. L. Sonnenberg, D. Williams-Young, F. Ding, F. Lipparini, F. Egidi, J. Goings, B. Peng, A. Petrone, T. Henderson, D. Ranasinghe, V. G. Zakrzewski, J. Gao, N. Rega, G. Zheng, W. Liang, M. Hada, M. Ehara, K. Toyota, R. Fukuda, J. Hasegawa, M. Ishida, T. Nakajima, Y. Honda, O. Kitao, H. Nakai, T. Vreven, K. Throssell, J. A. Montgomery, Jr., J. E. Peralta, F. Ogliaro, M. Bearpark, J. J. Heyd, E. Brothers, K. N. Kudin, V. N. Staroverov, T. Keith, R. Kobayashi, J. Normand, K. Raghavachari, A. Rendell, J. C. Burant, S. S. Iyengar, J. Tomasi, M. Cossi, J. M. Millam, M. Klene, C. Adamo, R. Cammi, J. W. Ochterski, R. L. Martin, K. Morokuma, O. Farkas, J. B. Foresman, and D. J. Fox, Gaussian 09, Revision E.01, Gaussian Inc. 2013.

[81] D. Feller, J. Chem. Phys. **96**, 6104 (1992).

[82] T. Helgaker, W. Klopper, H. Koch, and J. Noga, J. Chem. Phys. **106**, 9639 (1998).

[83] J. Pottel and N. Moitessier, J. Chem. Inf. Model. **57**, 454 (2017).

[84] C. Benecke, T. Gruer, A. Kerber, · R Laue, and T. Wieland, Fresenius J Anal Chem **359**, 23 (1997).

[85] R. Gugisch, A. Kerber, A. Kohnert, R. Laue, M. Meringer, C. Rucker, and A. Wassermann, (2009).

[86] J.M.L. Martin and G. de Oliveira, J. Chem. Phys. **111**, 1843 (1999).

[87] L. Deng, T. Ziegler, and L. Fan, J. Chem. Phys. **99**, 3823 (1993).

[88] K. Kim and K.D. Jordan, J. Phys. Chem. **98**, 10089 (1994).

[89] P.J. Stephens, F.J. Devlin, C.F. Chabalowski, and M.J. Frisch, J. Phys. Chem. **98**, 11623 (1994).

[90] S. Parthiban and J.M.L. Martin, J. Chem. Phys. **114**, 6014 (2001).

[91] R. Hadjadj, C. Deák, Á.B. Palotás, P. Mizsey, and B. Viskolcz, J. Clean. Prod. **241**, 118221 (2019).

[92] J. Tomasi, B. Mennucci, and R. Cammi, Chem. Rev. **105**, 2999 (2005).

[93] M. Cossi, N. Rega, G. Scalmani, and V. Barone, J. Comput. Chem. **24**, 669 (2003).

[94] V. Barone and M. Cossi, J. Phys. Chem. A **102**, 1995 (1998).

[95] X. Li and M.J. Frisch, J. Chem. Theory Comput. **2**, 835 (2006).

[96] E. Papajak, J. Zheng, X. Xu, H.R. Leverentz, and D.G. Truhlar, J. Chem. Theory Comput. **7**, 3027 (2011).

[97] R.J. Bartlett and G.D. Purvis, Int. J. Quantum Chem. **14**, 561 (1978).

[98] M.. McGlashan, Thermodynamic Properties of Individual Substances (Hemisphere Pub. Corp, New York :, 2004).

[99] E.U. Franck, Berichte Der Bunsengesellschaft Für Phys. Chemie **94**, 93 (1990).

[100] B. Ruscic, J.E. Boggs, A. Burcat, A.G. Császár, J. Demaison, R. Janoschek, J.M.L. Martin, M.L. Morton, M.J. Rossi, J.F. Stanton, P.G. Szalay, P.R. Westmoreland, F. Zabel, and T. Bérces, J. Phys. Chem. Ref. Data **34**, 573 (2005).

[101] B. Ruscic, R.E. Pinzon, M.L. Morton, N.K. Srinivasan, M.-C. Su, A. James W. Sutherland, and J. V. Michael, (2006).

[102] E.W. Lemmon, M.O. McLinden, and and D.G. Friend, NIST Chemistry WebBook, NIST Standard Reference Database (2017).

[103] A.J.C. Varandas, Annu. Rev. Phys. Chem. **69**, 177 (2018).

[104] A.F.G. Neto, F.C. Marques, A.T. Amador, A.D.S. Ferreira, and A.M.J.C. Neto, Renew. Energy **130**, 495 (2019).

[105] R. Hadjadj, I.G. Csizmadia, P. Mizsey, S.K. Jensen, B. Viskolcz, and B. Fiser, Chem. Phys. Lett. **746**, 137298 (2020).

[106] S.G. Jadhav, P.D. Vaidya, B.M. Bhanage, and J.B. Joshi, Chem. Eng. Res. Des. **92**, 2557 (2014).

[107] X. Jiang, X. Nie, X. Guo, C. Song, and J.G. Chen, Chem. Rev. acs. chemrev.9b00723 (2020).

[108] G. Righi, R. Magri, and A. Selloni, J. Phys. Chem. C **123**, 9875 (2019).

[109] T. Panczyk, P. Szabelski, and W. Rudzinski, J. Phys. Chem. B **109**, 10986 (2005).

[110] D.M. Weekes, D.A. Salvatore, A. Reyes, A. Huang, and C.P. Berlinguette, Acc. Chem. Res. **51**, 910 (2018).

[111] Y. Zheng, J. Wang, B. Yu, W. Zhang, J. Chen, J. Qiao, and J. Zhang, Chem. Soc. Rev. **46**, 1427 (2017).

[112] J.J. Kaczur, H. Yang, Z. Liu, S.D. Sajjad, and R.I. Masel, Front. Chem. **6**, 1 (2018).

[113] B. deB, Bond Dissociation Energies in Simple Molecules (n.d.).